Naval Research Laboratory
Washington, DC 20375-5320

NRL/MR/6176--97-7952

Enhancement to the ET-35N Oil Content Monitor: A Model Based on Mie Scattering Theory

R. L. MOWERY
H. D. LADOUCEUR
A. PURDY

Surface Chemistry Branch
Chemistry Division

June 6, 1997

REPORT DOCUMENTATION PAGE

Form Approved
OMB No. 0704-0188

1. AGENCY USE ONLY (*Leave Blank*)	2. REPORT DATE	3. REPORT TYPE AND DATES COVERED
	June 6, 1997	Interim Report, April 1996-April 1997

4. TITLE AND SUBTITLE

Enhancements to the ET-35N Oil Content Monitor:
A Model Based on Mie Scattering Theory

5. FUNDING NUMBERS

PE - 63721N

6. AUTHOR(S)

R.L. Mowery, H.D. Ladouceur, and A. Purdy

7. PERFORMING ORGANIZATION NAME(S) AND ADDRESS(ES)

Naval Research Laboratory
Washington, DC 20375-5320

8. PERFORMING ORGANIZATION REPORT NUMBER

NRL/MR/6176--97-7952

9. SPONSORING/MONITORING AGENCY NAME(S) AND ADDRESS(ES)

Commander, Naval Sea Systems Command (NAVSEA)
Attn: Joe Pizzino, Code 03R16
2531 Jefferson Davis Highway
Arlington, VA 22242-5160

10. SPONSORING/MONITORING AGENCY REPORT NUMBER

11. SUPPLEMENTARY NOTES

12a. DISTRIBUTION/AVAILABILITY STATEMENT

Approved for public release; distribution unlimited.

12b. DISTRIBUTION CODE

13. ABSTRACT (*Maximum 200 words*)

A theoretical model to calculate the turbidity of oil-in-water emulsions formed in the Navy's ET-35N Oil Content Monitor (OCM) has been developed. The model predicts that the turbidity measurements of the ET-35N will be dependent on the oil droplet size, the wavelength of the light used to illuminate the sample, and on the angle at which the light is scattered. It also shows that the turbidity is a linear function of oil concentration from 0 to 15 ppm but that the slope of the turbidity-concentration curve is oil droplet diameter dependent. The model also predicts that the turbidity decreases dramatically for oil droplets less than 0.2 μ in size implying that the ET-35N is not very sensitive to oil-in-water emulsions containing droplets of this diameter or less. The model suggests modifications to the ET-35N which should increase its sensitivity by a factor of three and a modification that will reduce the turbidity's dependence on the diameter of the oil droplets being analyzed thus improving the accuracy of the turbidity measurements.

14. SUBJECT TERMS

Turbidity
Oil content monitor
Light scattering
Mie modeling

15. NUMBER OF PAGES

49

16. PRICE CODE

17. SECURITY CLASSIFICATION OF REPORT	18. SECURITY CLASSIFICATION OF THIS PAGE	19. SECURITY CLASSIFICATION OF ABSTRACT	20. LIMITATION OF ABSTRACT
UNCLASSIFIED	UNCLASSIFIED	UNCLASSIFIED	UL

NSN 7540-01-280-5500

Standard Form 298 (Rev. 2-89)
Prescribed by ANSI Std 239-18
298-102

CONTENTS

1. INTRODUCTION 1

2. TURBIDITY MEASUREMENT ENHANCEMENTS 1

2.1 Background 1
2.2 Approach 4
2.3 Scattering Calculations 5
2.4 Results of the Turbidity Calculations 9
2.5 Discussion 29
2.6 Conclusions 37
2.7 Recommendations 42

3. FURTHER MODELING WORK 43

4. REFERENCES 44

5. APPENDIX 45

ENHANCEMENTS TO THE ET-35N OIL CONTENT MONITOR: A MODEL BASED ON MIE SCATTERING THEORY

1 Introduction

1.1 The U.S. Navy is developing/adopting appropriate technologies for oil pollution abatement aboard ships to meet stricter standards being imposed by federal and local agencies. Standards that specify the level of oil that can be discharged from the bilge of vessels both at sea and in port have recently been or are expected to be lowered to 5 ppm. In order to meet these lower levels the U.S. Navy has determined that its present OCM, oil content monitor, which can measure oil levels down to 15 ppm, may not be accurate enough to assure compliance with the new standards. Thus the Naval Research Laboratory (NRL) has been tasked to investigate alternative technologies that could meet the U.S. Navy's need for a more accurate OCM.

1.2 Two of the alternative approaches being explored are
a) Turbidity Measurement Enhancements to the present OCM
and
b) Alternative Coatings for a Fiber Optic/Optical Wave guide OCM Probe (WOP).

1.3 This report gives the results of scattering calculations modeling the measurements made by the present Navy OCM to test the feasibility of improving its sensitivity and/or accuracy.

2 Turbidity Measurement Enhancements

2.1 Background

2.1.1 The present method used in the Navy's OCM is based on turbidity measurements of a bilge water sample. The turbidity of the water sample can be determined by measuring both the attenuation of the intensity of a beam of light passing through a sample of water and the intensity of the light that is scattered by the water sample. The attenuation of the light beam can be caused both by absorption and by scattering of the light.

2.1.2 Specifically the turbidity measurements on most Navy vessels are made by the ET-35N an automated OCM. This device uses a chamber which can capture and isolate a bilge water sample from the effluent stream leaving the OWS (oil/water separator) or the secondary oily waste treatment system (SOWTS). Photographs and schematics of the ET-35N can be found in reference 1. The oil content measurement incorporates the series of steps (2.1.2a - 2.1.2g) outlined below:

Manuscript approved April 24, 1997

2.1.2a A bilge water sample is admitted to the sampling chamber of the ET-35N (see Fig. 2.1.2a).
2.1.2b The sample is subjected to a 1 sec low frequency (5 kHz) sonification step to remove gas bubbles (debubble) the sample.
2.1.2c Separate light intensity measurements are made by two photodiodes embedded in the optical sensor ring, OSR (see Fig. 2.1.2c). The first intensity measurement is made by a photodiode that is positioned opposite the LED (red) in the sensor ring (a 0^{o} measurement from the forward propagation direction). This measurement provides the attenuation of the light by the bilge water sample. The second intensity measurement is made by a photodiode that is positioned approximately 45^{o} from the first photodiode (a 45^{o} measurement). This measurement yields the intensity of the light that has been scattered by particulates, including oil droplets, in the bilge water sample. The first measurement is divided into the second measurement to obtain a turbidity reading.
2.1.2d The sample is subjected to a 5 sec 50 kHz sonification step to emulsify the oil in the sample.
2.1.2e The sample is subjected to a 1 sec low frequency (5 kHz) sonification step to debubble the sample.
2.1.2f The third and forth light intensity measurements are made. These measurements are made as before, at 0^{o} and at 45^{o} and the two measurements are ratioed to give a second turbidity reading.
2.1.2g The bilge water in the sampling chamber is replaced by a new sample taken from the effluent stream from the OWS or the SOWTS and the measurement cycle is started over. The whole sampling cycle takes about 15 s.

2.1.3 The two turbidity readings (at 0^{o} and 45^{o}) are compared in order to determine the increase in turbidity that occurred before and after the bilge water sample was emulsified. This comparison allows a correction to be made for solid particulates (dirt, for example) that would contribute to the scattered light at 45^{o}. This corrected turbidity signal is then compared electronically to reference signals that represent oil in water concentrations of 15 ppm or 70 ppm (there are two ranges on the ET-35N) and an oil content reading is displayed.

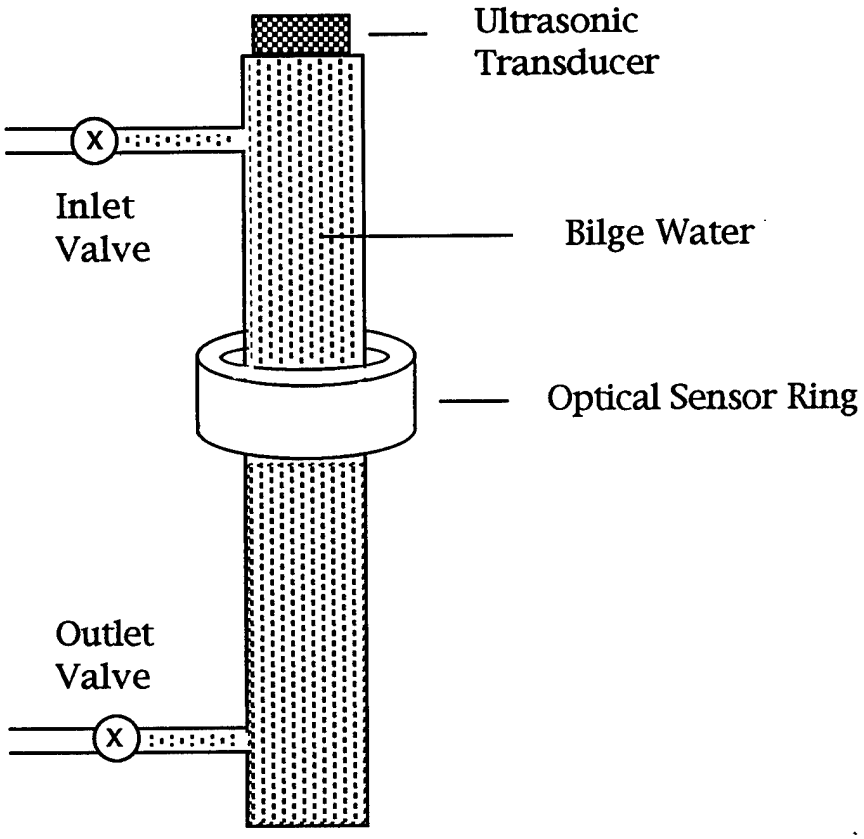

Figure 2.1.2a Simplified schematic of the ET-35N analysis cell. The transducer is used to debubble and emulsify the sample. The optical sensor ring (OSR) contains the LED light source and the photodetectors.

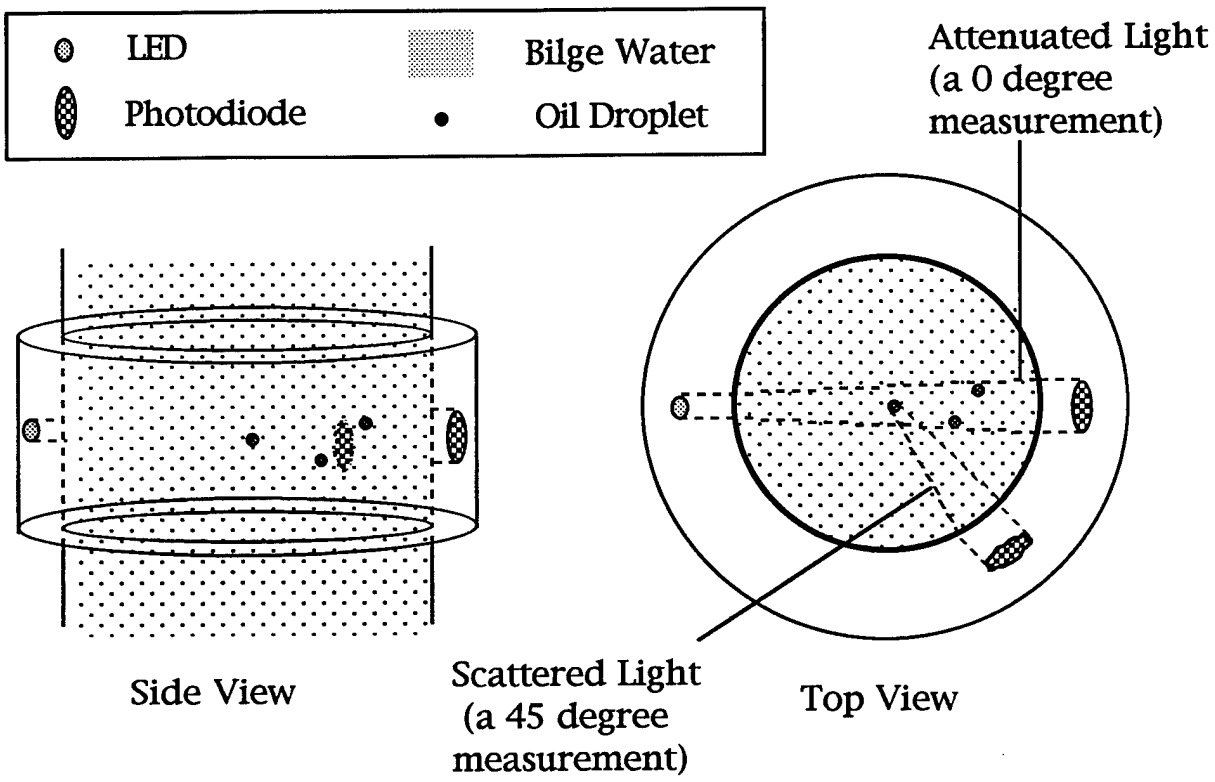

Optical Sensor Ring, ET-35N

Figure 2.1.2c Schematic of the optical sensor ring (OSR) of the ET-35N OCM. The analysis cell passes through the ring and the ring contains the LED light source and the photodetectors all of which are recessed into the OSR. An additional test LED is not shown in the schematic for simplicity.

2.2 Approach

Since the ET-35N depends on the scattering of light in order to measure turbidity, it should be possible to improve the accuracy and/or the sensitivity of the device by modifying the test conditions used for the light scattering measurements. Two relatively easy changes that could be made are:

2.1.2a. The wavelength of the light used to illuminate the bilge water sample could be changed or multiplexed - use two or more wavelengths of light to measure the turbidity.

2.1.2b. The angle at which the scattered light is observed (45^{o}) could be changed.

Theoretical calculations to determine the effect of changing these two test conditions on the scattering intensity by oil droplets in water were performed.

2.3 Scattering Calculations

2.3.1a As was noted in 2.1.2 the turbidity is the ratio of the light intensity of the light seen by the detector at 0^o to the intensity seen by the detector at 45^o (see Fig. 2.1.2c). Thus two scattering calculations must be done, one for the 0^o detector and one for the 45^o detector. These scattering calculations were done using the Mie theory which is a rigorous mathematical treatment of an electromagnetic plane wave (light) interacting with an isolated spherical particle[2]. The Mie theory provides both the scattering and the absorption cross sections for the suspended particles as functions of light wavelength, particle size and the bulk optical properties of the scattering system. If the average distance between particles (oil droplets) is roughly three times the particle radius, the scattering process is independent of a particle's location relative to other particles.[3] Thus the light intensities seen by the detectors from an ensemble of particles is the sum of the light intensity scattered by the individual particles. This is referred to as independent scattering. However, one must consider the location of the scattering particle relative to the detector since the angular distribution of the scattered light is not isotropic. The light scattered by an isolated spherical particle has an angular distribution which depends upon the particle's radius, the wavelength, the polarization of the light, and the optical properties of the particle (essentially its complex index of refraction). In the limit of large particles relative to the wavelength of the light, the angular distribution of scattered light tends to be in the forward or reverse direction (a scattering angle of $< 15^0$ or $> 150^o$). If the particles have diameters much less than the wavelength of the light, the scattering can be isotropic (no angular dependence). Thus a precise analysis of the intensity of the light seen by the detectors requires an accurate representation of the angular scattering distribution function as well as scattering cross sections and the number density of the scattering particles.

2.3.1b The mathematical formulae for the scattering derived from the Mie treatment are quite complicated involving infinite sums of Bessel functions and Legendre polynomials. However these infinite sums converge reasonably rapidly and can be evaluated accurately by computer. We have used FORTRAN code, documented in an IBM Palo Alto Scientific Center

report,[4] to calculate efficiency factors for extinction, Q, scattering, Q_s, and absorption, Q_a This code has been modified and compiled to run on a 486 or 586 class PC with Lahey FORTRAN 90 . The efficiency factor is the ratio of the scattering or absorption cross section to the particle's projected area. As the light from the LED traverses the sample cell it is absorbed and scattered. Measurements of the light intensity at 0^o can be related to an extinction cross section which includes the effects of both scattering and absorption. If the particles do not absorb the light, their index of refraction is real and the extinction cross section for the particles equals the scattering cross section.

2.3.2 For the 0^o detector the calculated Q relates the intensity, $I(0^o)$, of the light attenuated by scattering and observed by the detector (the 0^o measurement) to that of the intensity of the incident light, I_o, (from the LED) by the expression

$$I(0^o)=I_o \exp(-g\, l_o) \qquad \text{Eqn 2.3.2.1}$$

where

$$g= N \pi a^2 Q \qquad \text{Eqn 2.3.2.2}$$

and N is the number density in particles (or droplets)/unit volume, a is the radius of the particle or droplet, and l_o is the pathlength of the light in the medium (water, in our case) in the analysis cell.

2.3.3 Q depends upon several physical characteristics of the scattering system: a) The wavelength of the incident light that is being scattered; b) the index of refraction (real or complex) of the particle that is scattering the light; c) the index of refraction (real or complex) of the medium in which the particles are suspended; and, d) the radius of the particles (oil droplets).

2.3.4 For the 45^o detector, an expression relating the intensity, $I(\emptyset)$, of the light scattering into the detector to that of the incident light, I_i, falling upon an small scattering volume of bilge water containing oil droplets is necessary. It is given by

$$I(\emptyset)=I_i\, g\, P(\emptyset)/r^2, \qquad \text{Eqn 2.3.4}^{5}$$

where I_i (= $I_o \exp(-g\, l)$) accounts for the fact that the incident light striking an oil drop is attenuated by the scattering and absorption of all the

oil droplets between the illuminating LED and the oil droplet (at a distance l) that is scattering the light. g is given by Eqn 2.3.2.2 and P(Ø) is a normalized phase function derived from the Mie calculations. P(Ø) depends upon Ø, the scattering angle, and upon the physical characteristics listed in section 2.3.3. r is the distance from the scattering oil droplet to the 45^{o} detector

2.3.5 The use of Eqn. 2.3.4 in calculating the intensity of the scattered light into the 45^{o} detector is considerably more complicated than the calculation for the 0^{o} detector because:

a) An oil particle will scatter the light into the 45^{o} detector at an angle which varies with the position of the oil particle along the light path from the LED to the opposite side of the sample cell (see Fig. 2.3.5). P(Ø), which is the angular dependent term of Eqn. 2.3.4, can vary by an order of magnitude or more depending upon the angle Ø and thus the change in scattering due to the oil droplet's position in the cell should be incorporated into any theoretical calculation of turbidity.

b) Each oil particle sees a light intensity which varies with the distance of the oil particle along the light path from the LED to the opposite side of the sample cell, the I_i term of Eqn. 2.3.4. This is due to attenuation of the light from the LED by other oil droplets (and other scatterers) in the light path from the LED to the oil particle.

and

c) Any scattered light decreases in intensity as $1/r^2$, the distance from the scattering oil droplet to the 45^{o} detector. This is due to the fact that the scattering oil droplet can be considered as a point light source. The distance r varies with the position of the oil particle along the light path from the LED to the opposite side of the sample cell (see Fig. 2.3.5).

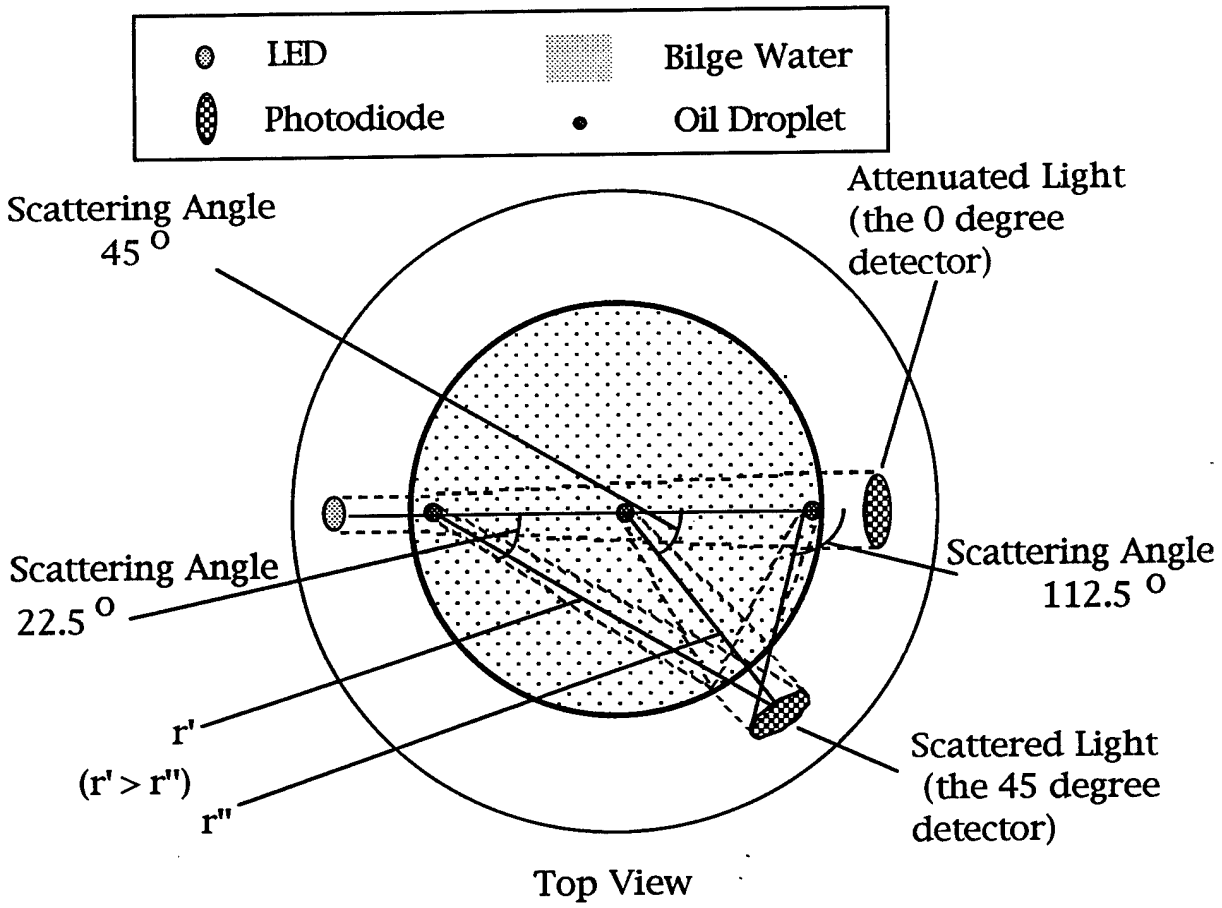

Optical Sensor Ring, ET-35N

Figure 2.3.5 Schematic of the optical sensor ring (OSR) of the ET-35N OCM. The diagram shows how the position of the oil droplet along the light beam of the LED changes the scattering angle into, and the distance to, the 45° detector.

2.3.6 The theoretical turbidity at any single scattering angle can then be calculated from Eqn. 2.3.2.1 and Eqn. 2.3.4 and results in an expression

$$T(\emptyset) = I(\emptyset)/I(0) = \exp(-g(l-l_o))\ g\ P(\emptyset)/r^2 \qquad \text{Eqn 2.3.6}$$

where $\emptyset$ is the scattering angle, l is the distance from the LED to the scattering droplet, l_o is the diameter of the OCM analysis cell and r is the distance from the scattering oil droplet to the 45° detector.

2.4 Results of the Turbidity Calculations

2.4..1 Turbidity calculations were done for a variety of wavelength of incident light and for a range of oil droplet sizes. The droplets are assumed to be non-absorbing at the wavelength of light used to illuminate the sample and are assumed to have an index of refraction of 1.5. Since the scattering angle is dependent upon the position of the oil particle in the LED beam path in the analysis cell two "limiting" positions for the scattering oil droplets were chosen. The first position was chosen to be at the wall of the analysis cell next to the LED. This point was chosen because it results in the lowest scattering angle, 22.5°, and the term P(Ø), which contributes to the turbidity (see Eqn. 2.3.6), increases as the scattering angle, Ø, gets smaller. In addition, scatterers at this point see the full intensity of the light from the LED, i.e., no attenuation of the illuminating light occurs.

2.4.2 The second position was chosen at the center of the analysis cell. Although this point exhibits a scattering angle of 45° and thus a smaller value of P(Ø), the geometric collection efficiency of the 45° detector is maximum for droplets scattering light from this position. Also, oil droplets scattering from this position are closer to the 45° detector then droplets located nearer to the LED (see Fig. 2.3.5). Scatterers that are closer to the 45° detector increase the $(1/r^2)$ term in Eqn. 2.3.6 and, consequently, increase the calculated turbidity.

2.4.3 Oil droplets beyond the center of the analysis cell in the LED beam path contribute less and less to the turbidity because the scattering angle for these droplets exceeds 45° and the phase function, P(Ø) gets smaller as the scattering angle increases. In addition, the geometric collection efficiency of the 45° detector decreases as the scattering exceeds 45°. Thus the contribution to the turbidity of particles beyond the center of the cell are ignored in these calculations.

2.4.4 The scattering calculations were done assuming a uniform oil emulsion between the limiting positions in the analysis cell described above. The oil-in-water emulsion was divided into 150 volume elements beginning at the sample cell's wall next to the LED and ending at the center of the sample cell. The scattering into the 45° detector was calculated for each volume element and the contribution from each volume element was summed to approximate the total scattering, T, into the 45° detector.

$$T = \sum_i \exp(-g(l_i - l_0))\ g\ P(\emptyset_i)/r_i^2 \quad (i=1,150) \qquad \text{Eqn 2.4.4}$$

The oil droplets were assumed to be spherical in shape and of uniform diameter. Under these assumptions, the number density, N, which is needed for the calculation of g, can be calculated if the density of the oil and the concentration (in ppm) of the emulsified oil is set. The droplets were assumed to be composed of a water-immiscible oil with a real index of refraction of 1.5 (common for most hydrocarbons in the wavelength region studied) and a density of 0.87g/mL at room temperature. These properties closely mimic those of Navy test standard, oil mix #4, (OM#4) which is a mixture of 25% MS-2190-TEP (MIL-L-17331), 25% MS-9250 (MIL-L-9000) and 50% diesel fuel marine (DFM). The percentages are by weight. The index of refraction for the bilge water was assumed to be that of pure water and was near 1.33 for all the wavelengths studied. The parameters used in the turbidity calculations are summarized in Table 2.4.4

Parameter	Value
Index of Refraction of Bilge water	≈ 1.3
Index of Refraction of Oil	1.5
Oil Droplet Shape	Spherical
Oil Droplet Density	0.87 g/mL
Analysis Cell Path Length	1.1 cm
Scattering Angle	22.5^o -> 45^o
Oil Droplet Diameter	0.1 - 2.0 μ
Conc. of Oil Emulsion	1,5,15 &30 ppm
LED Wavelength	0.45 - 2.2 μ

Table 2.4.4 The values of the parameters used in the bilge water oil emulsion turbidity calculations. Those parameters that were varied during the calculations are at the bottom of the table.

2.4.5 The calculated turbidity for an oil-in-water emulsion verses droplet size is shown in Fig. 2.4.5a. The wavelength of the incident light is 0.65 μ, which should be near the wavelength of the red LED presently used in the OSR of the ET-35N. The graph shows that the turbidity is very droplet size dependent. Droplets with a diameter near 0.7 μ have a turbidity twice that of particles with a diameter of less than 0.4 μ or greater than 1.1 μ. This behavior is even more pronounced if the wavelength of the incident light is shorter (see Fig. 2.4.5b) and diminishes if wavelengths longer than 0.65 μ are used (Fig. 2.4.5c).

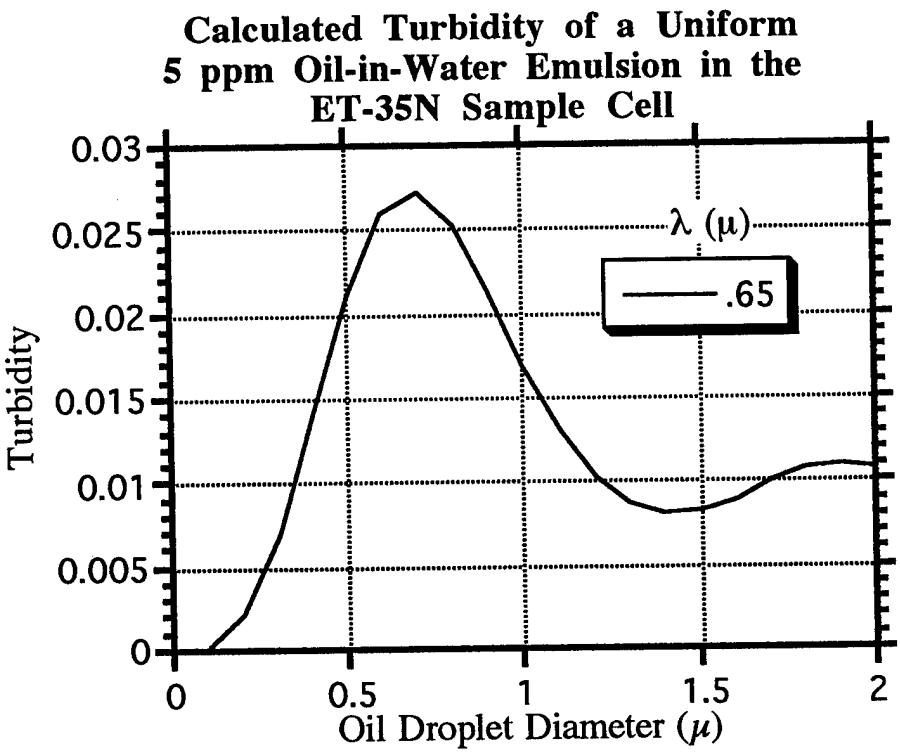

Figure 2.4.5a. Calculated turbidity versus oil droplet diameter using Eqn 2.4.4. The calculation is based on a uniform oil droplet size for each droplet diameter and is for a 5 ppm oil-in water emulsion.

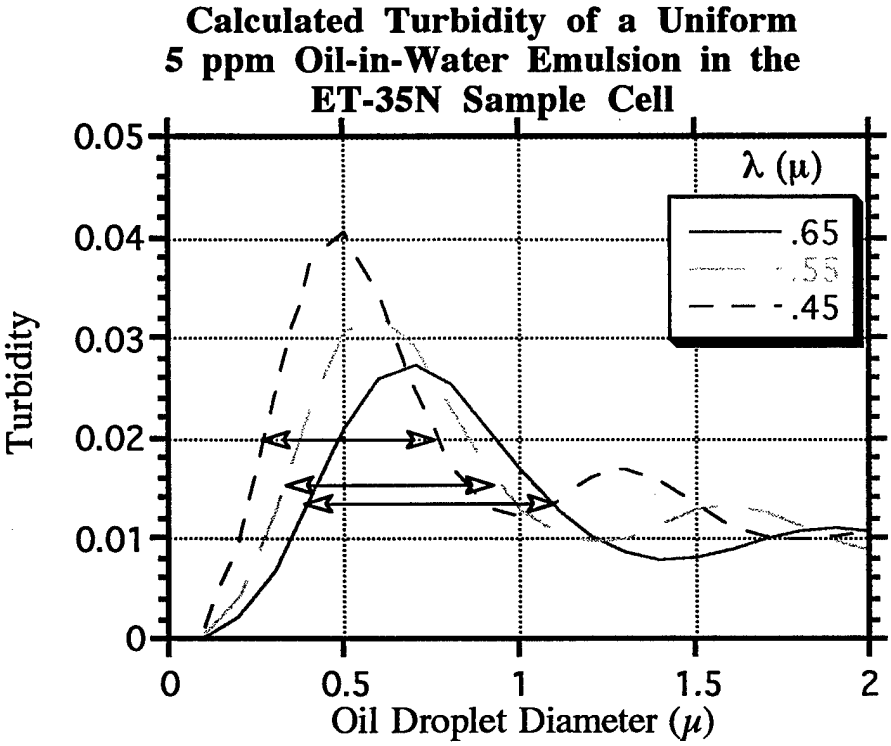

Figure 2.4.5b. Calculated turbidity versus oil droplet diameter at various incident light wavelengths (<= 0.65 μ). The calculation is based on a uniform oil droplet size for each droplet diameter and is for a 5 ppm oil-in water emulsion. The double headed arrows show the range of particle diameters that exhibit turbidity more than 1/2 of the peak turbidity for a particular incident light wavelength. These ranges narrow as the incident light wavelength gets shorter.

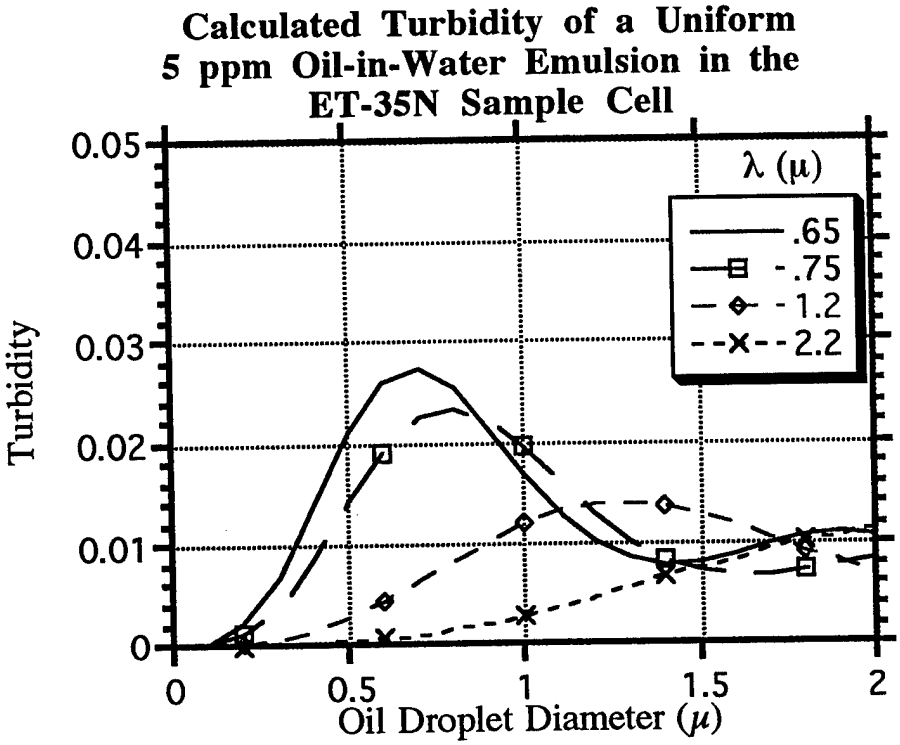

Figure 2.4.5c. Calculated turbidity versus oil droplet diameter at various incident light wavelengths (=> 0.65 μ). The calculation is based on a uniform oil droplet size for each droplet diameter and is for a 5 ppm oil-in-water emulsion. The dependence of turbidity on particle diameter decreases as the incident wavelength increases.

2.4.6 The turbidity calculations were done for a series of concentrations (in ppm oil) and the results at various concentrations and for a variety of incident light wavelengths are shown in Fig. 2.4.6a-c. The figures show that the calculated turbidity curves at a single wavelength have the same general shape but differ in magnitude as would be expected. These figures and Fig. A-1 to A-5 in the appendix also show that the maximum turbidity at any one wavelength of light occurs at nearly the same oil droplet size irrespective of the concentration of the oil-in-water emulsion. This observation holds at least in the range of concentrations from 0 to 30 ppm.

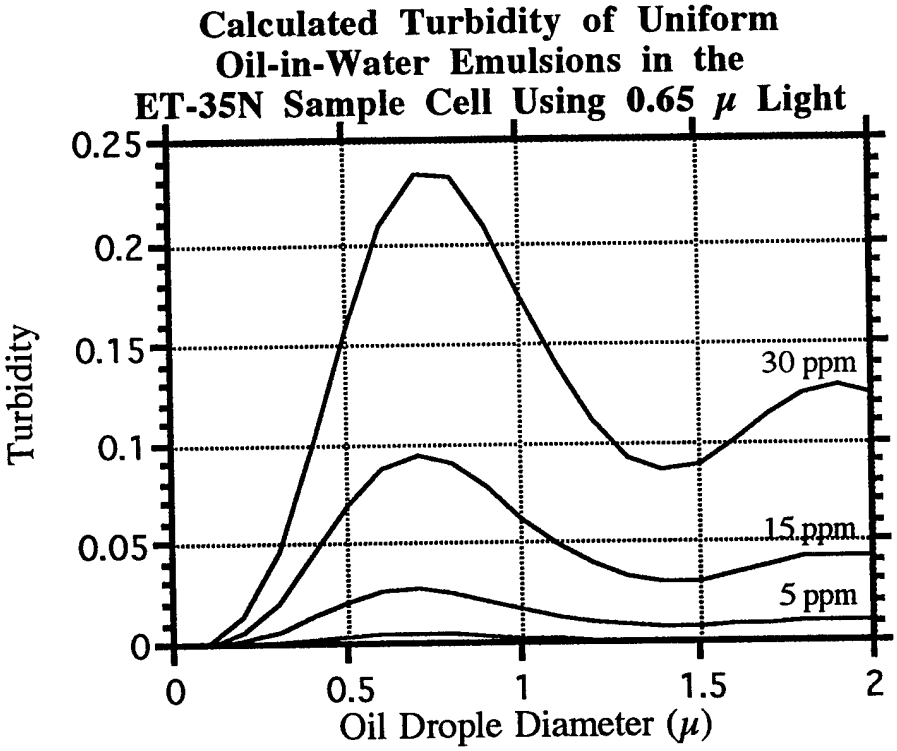

Figure 2.4.6a. Calculated turbidity versus oil droplet size using Eqn 2.4.4. The calculation is based on a uniform oil droplet size for each droplet diameter and is for 1 ppm (lowest curve), 5 ppm, 15 ppm and 30 ppm oil-in water emulsions. The wavelength of the illuminating light is 0.65 μ which is close to that used in the ET-35N OSR.

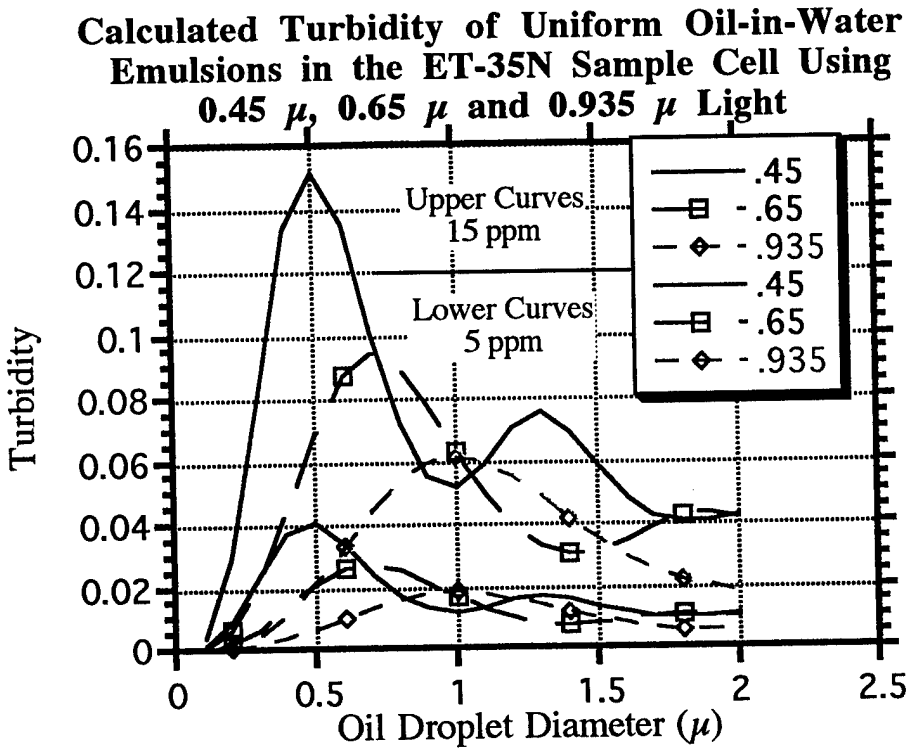

Figure 2.4.6b. Calculated turbidity versus oil droplet size using Eqn 2.4.4. The calculation is based on a uniform oil droplet size for each droplet diameter and is for a 5 ppm and a 15 ppm oil-in water emulsion illuminated by three different wavelengths of light. Curves of the same color and line style are calculated turbidities at the same wavelength of light but at the two different emulsion concentrations.

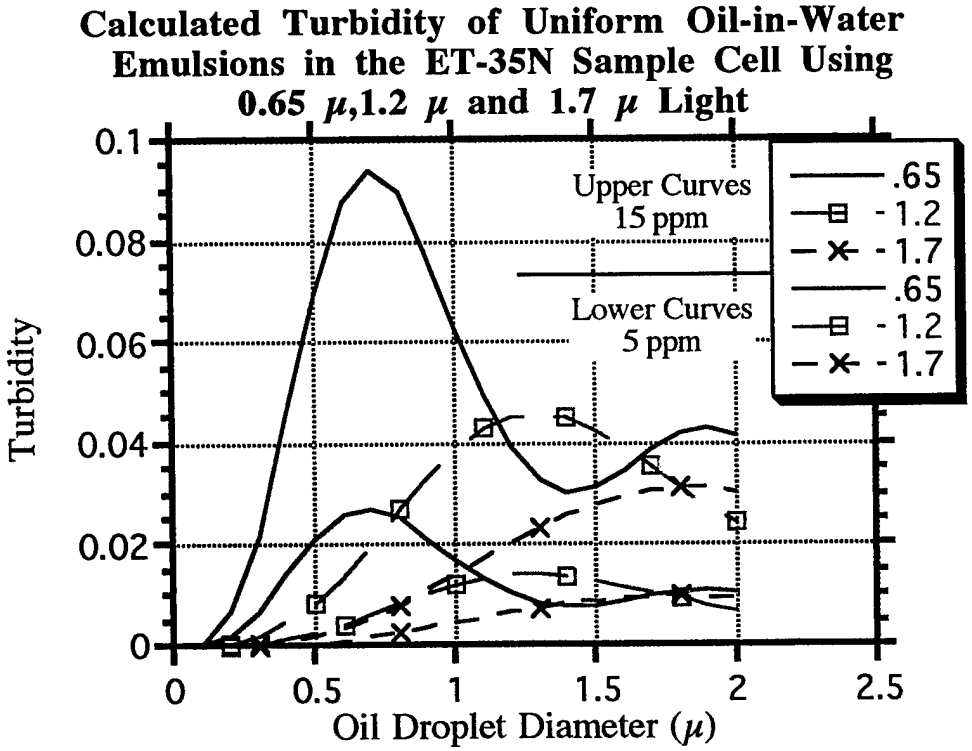

Figure 2.4.6c. Calculated turbidity versus oil droplet size using Eqn 2.4.4. The calculation is based on a uniform oil droplet size for each droplet diameter and is for a 5 ppm and a 15 ppm oil-in water emulsion illuminated by to different wavelengths of light. Curves of the same color and line style are calculated turbidities at the same wavelength of light but at the two different emulsion concentrations.

2.4.7a All of the above turbidities were calculated using the 0° (attenuated light) and 45° (scattered light) detector configuration found in the ET-35N analysis cell. Additional turbidity calculations were done by holding the position of the 0° detector fixed and changing the position of the other detector on the optical sensor ring so that the angle between the detectors varies between 5° to 170°. Equation 2.4.4 was modified to accommodate this variation on the angle between the detectors and can be expressed as

$$T(ß) = \sum_i \exp(-g(l_i - l_0))\ g\ P(ø_i(ß))/r_i^2 \quad (i=1,150) \qquad \text{Eqn 2.4.7a,}$$

where ß is the angle between the detectors and $ø_i(ß)$, the scattering angle, will vary between limits that will depend upon ß. A calculated angle-between-detectors vs. turbidity plot for incident light at 0.65 μ is shown in Fig. 2.4.7a. Additional plots of the angular dependence of the turbidity for

other wavelengths of incident light are shown in the appendix as Fig. A-6 through A-11.

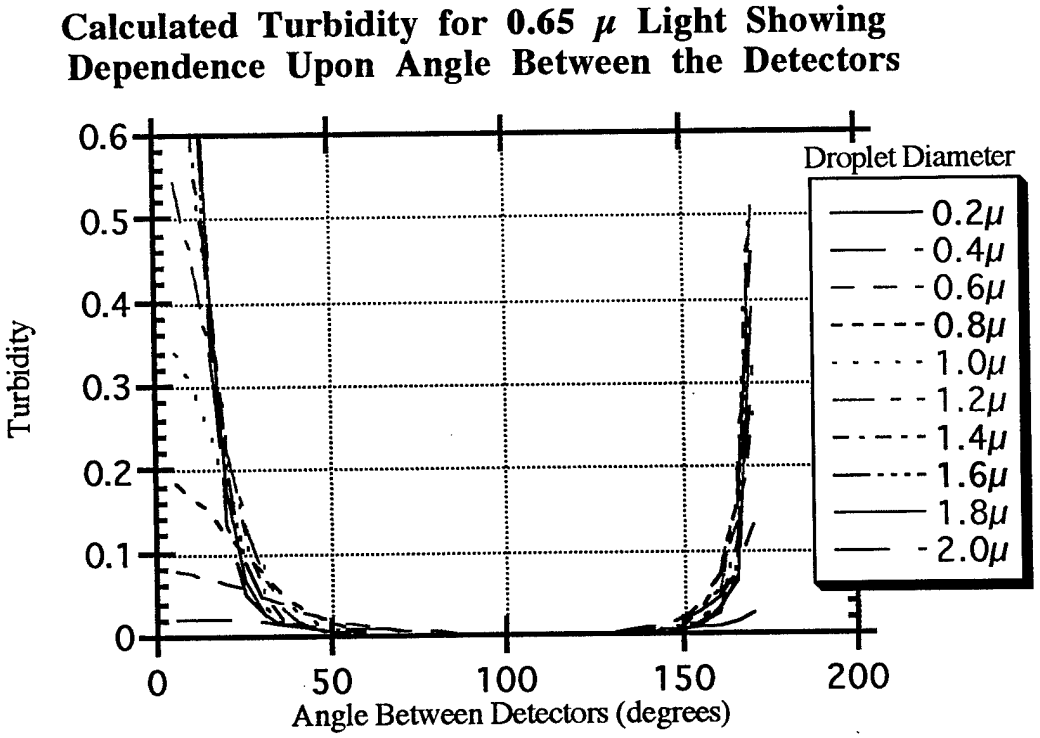

Figure 2.4.7a. Calculated turbidity versus angle between the attenuated and scattered light detectors at various oil droplet sizes based on Eqn 2.4.7a. The calculation assumes a uniform oil droplet size for each droplet diameter and is for a 5 ppm oil-in water emulsion illuminated by 0.65 μ light.

2.4.7b All of the angle-between-detectors vs. turbidity plots have the same general shape. The turbidity is high at very small angles (< 30°) but it decreases to values on the order of 1/100 of the maximum turbidity for a wide range of angles (50° to 150°). The turbidity then increases by about an order of magnitude as the angle between the detectors approaches 180°. The wavelength dependence of the turbidities does, however, vary somewhat with angle between the detectors. At low angles (<30°) the turbidity has a value near 2.5 at a wavelength of 0.45 μ and then decreases by a factor of approximately 40 as the illuminating light's wavelength increases from 0.45 μ to 1.7 μ (see Fig. 2.4.7b-1). A similar but less dramatic trend is exhibited by the turbidities at high angles (>150°). The turbidities approach a value of 0.15 at a wavelength of 0.45 μ and then decrease by roughly a factor of four as the illuminating light's wavelength

increases from 0.45 μ to 1.7 μ (see Fig. 2.4.7b-2). At intermediate angles (50^0 to 150^o) the turbidities lie below a value of 0.003 for almost all wavelengths and almost all oil droplet sizes spanned in the calculations.(see Fig. 2.4.7b-3). For reference, a plot of the wavelength dependence of the turbidities at an angle of 45^o between the detectors, which is the optical configuration found in the ET-35N OCM, is shown in the appendix as Fig. A-12.

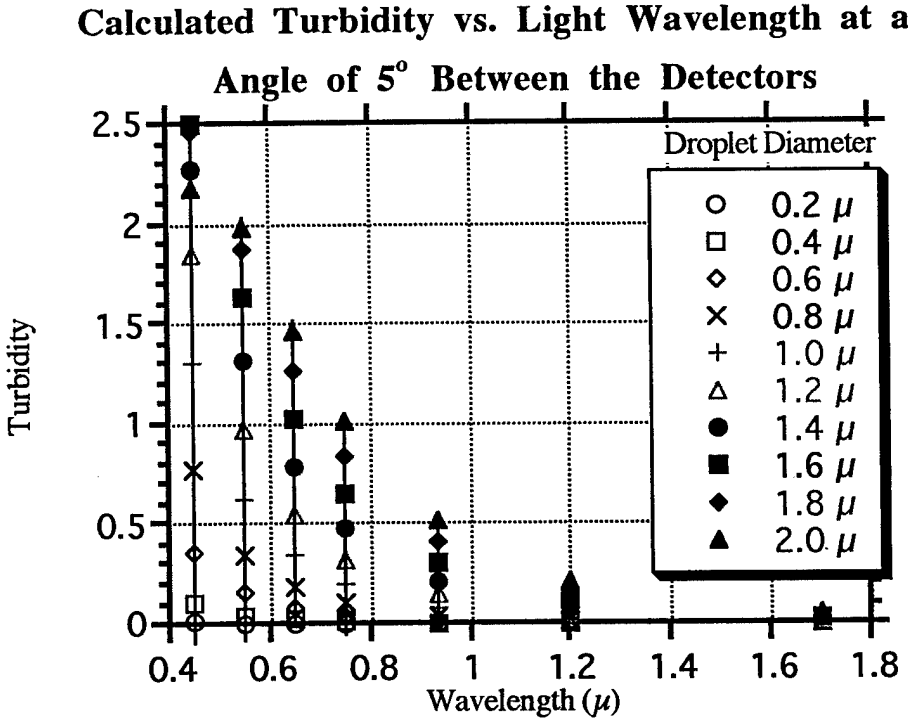

Figure 2.4.7b-1. Calculated turbidity versus wavelength of the illuminating light at a fixed angle between the attenuated and scattered light detectors. The calculation assumes a uniform oil droplet size for each droplet diameter and is for a 5 ppm oil-in water emulsion.

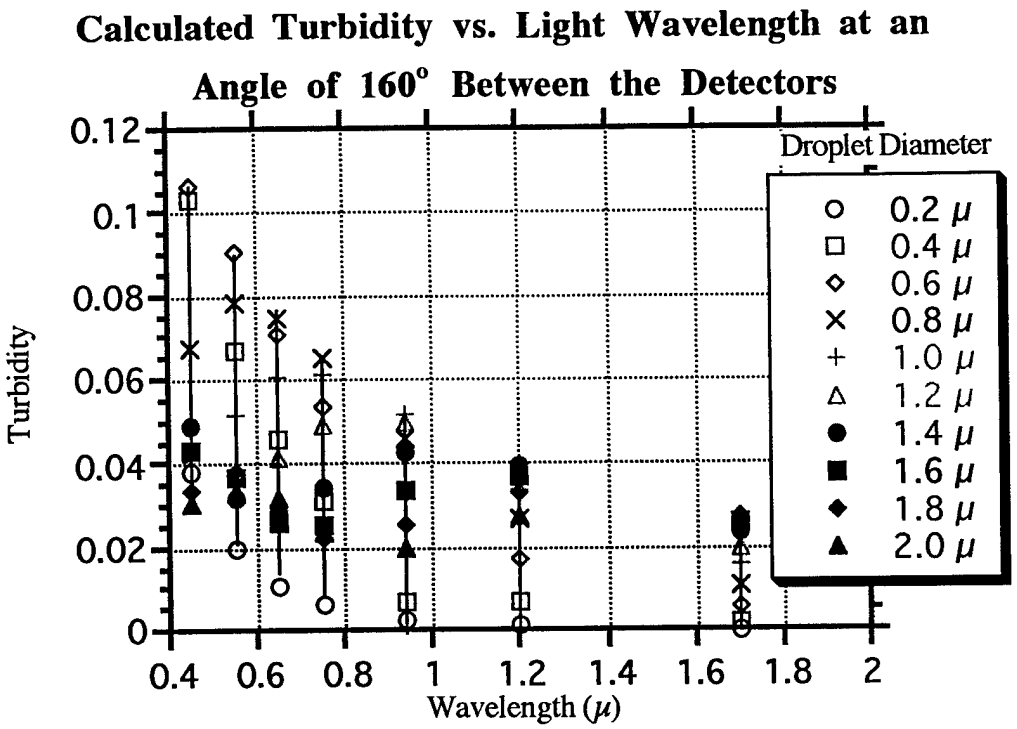

Figure 2.4.7b-2. Calculated turbidity versus wavelength of the illuminating light at a fixed angle between the attenuated and scattered light detectors. The calculation assumes a uniform oil droplet size for each droplet diameter and is for a 5 ppm oil-in water emulsion.

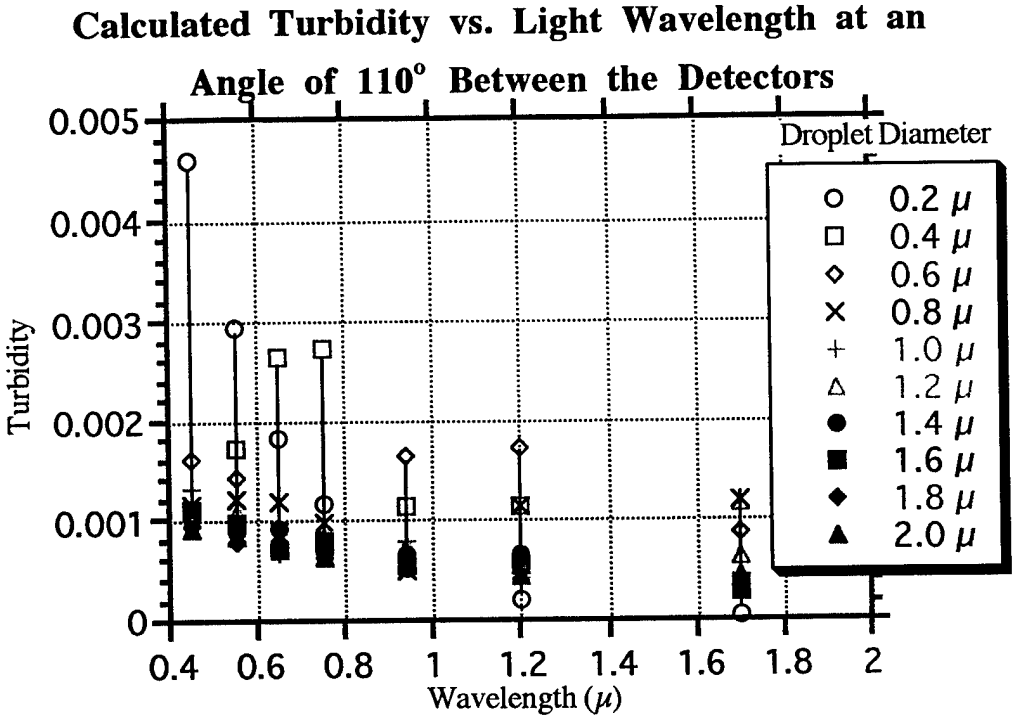

Figure 2.4.7b-3. Calculated turbidity versus wavelength of the illuminating light at a fixed angle between the attenuated and scattered light detectors. The calculation assumes a uniform oil droplet size for each droplet diameter and is for a 5 ppm oil-in water emulsion.

2.5 Discussion

2.5.1 From the results of the turbidity calculations for the ET-35N OCM shown in the previous section, it can be seen that there is a maximum in the turbidity (T_m) versus oil droplet size curve. The droplet size at which this maximum occurs and the magnitude of T_m varies with the wavelength of the light used to illuminate the oil-in-water emulsion. Figure 2.5.1a illustrates how the oil droplet size at the maximum turbidity varies with wavelength. It is a linear relationship and, within the uncertainty in identifying the maximum in the turbidity introduced by the finite step size in droplet diameter used in the turbidity calculations, the relationship is: The oil droplet diameter which results in the maximum turbidity is approximately equal to the wavelength (in air) of the light used to irradiate the sample. This relationship is very useful since it allows us to choose an approximate optimal wavelength to use for measuring the turbidity of an oil-in-water emulsion of a particular oil droplet size.

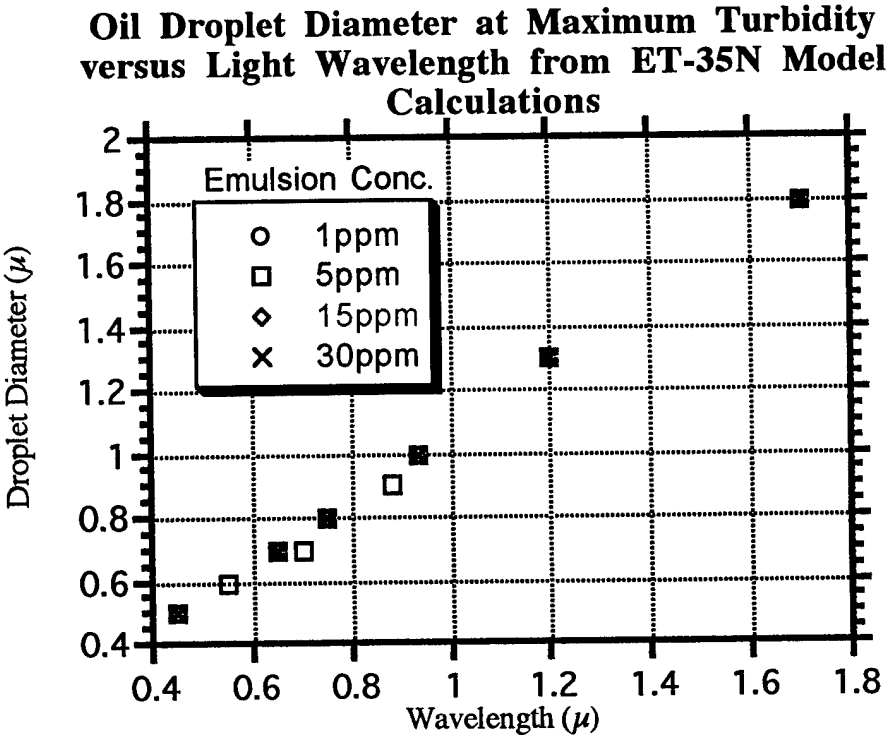

Figure 2.5.1a. Plot of the oil droplet diameter at the maximum turbidity versus illuminating wavelength in air for the ET-35N. The calculation is based on a uniform oil droplet size for each droplet diameter and includes 1, 5, 15 and 30 ppm oil-in-water emulsions. The droplet size at T_m appears to vary linearly with wavelength.

Another result of the model calculations is that the maximum value of the calculated turbidity shows a monotonic decrease as the wavelength of the irradiating light increases. This is shown in Fig. 2.5.1b. The implication here is that if we have a uniform or near uniform distribution in oil droplet sizes in the analysis cell we should choose the shortest feasible wavelength of light to illuminate the sample. Such a choice will maximize the turbidity signal.

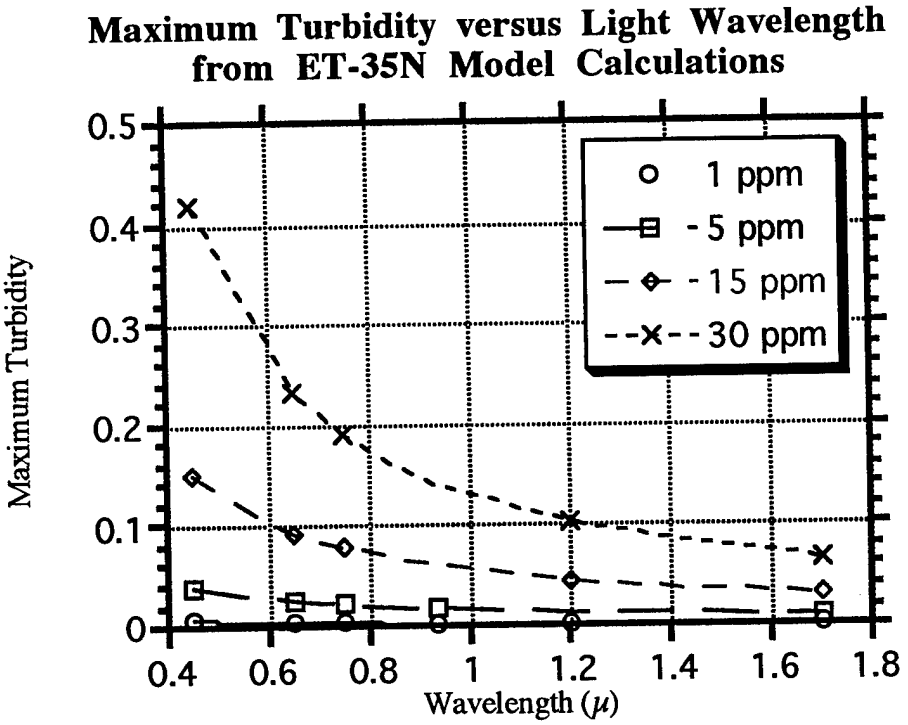

Figure 2.5.1b. Plot of the maximum turbidity (T_m) versus illuminating wavelength in air for the ET-35N. The maximum turbidities were derived from turbidity vs. oil droplet diameter plots at a set wavelength of light using Eqn. 2.4.4. T_m decreases with increasing wavelength for all the oil emulsion concentrations considered.

2.5.2a The concentration dependence of the turbidity can be derived from the model calculations. Consideration of the curves shown in Fig. 2.4.6a indicate that the turbidity is not linear with oil emulsion concentration (see Fig. 2.5.2a). For emulsion concentrations less than about 15 ppm the turbidity vs. concentration curves are nearly linear for droplet sizes less than 2.0 micron in diameter (see Table 2.5.2b. Above 15 ppm the curves deviate from linearity with an upward bias.

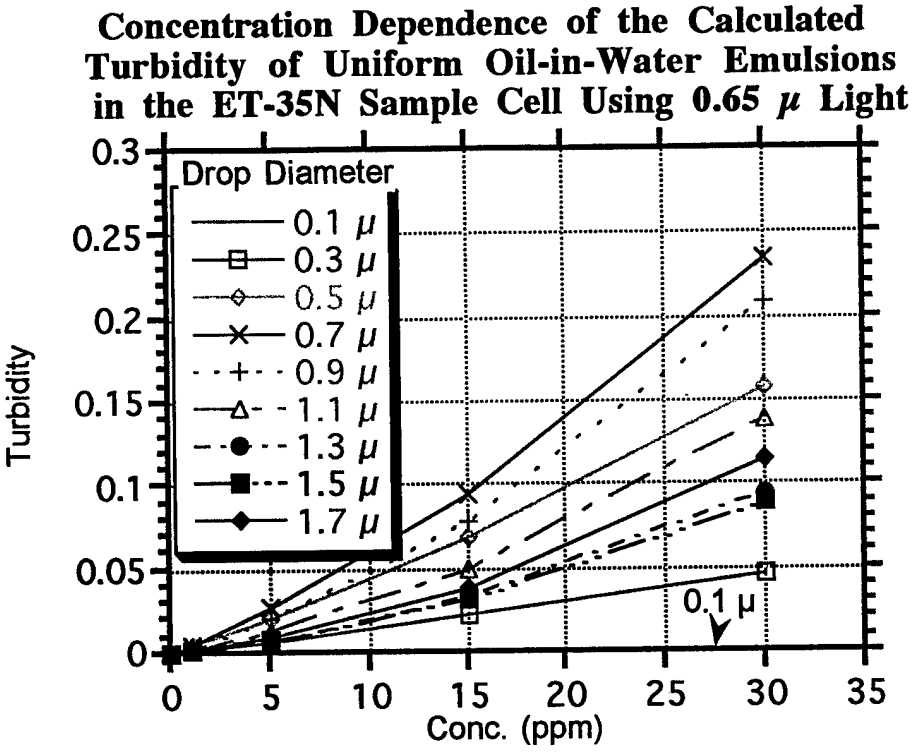

Figure 2.5.2a. Calculated turbidity versus oil concentration using Eqn 2.4.4 and based on the optical configuration of the ET-35N analysis cell. The calculations assume a uniform oil droplet diameter at each droplet diameter and is for 1 ppm, 5 ppm, 15 ppm and 30 ppm oil-in-water emulsions.

2.5.2b The concentration dependence of the turbidities from the model calculations also show that the slope of the turbidity vs. concentration curve varies with oil droplet diameter. This can be seen from the curves displayed in Fig. 2.5.2a and can be quantified by doing a least squares fit to the calculated turbidities from 0 to 15 ppm. The results of these fits are given in Table 2.5.2b The variation of slope with oil droplet diameter implies that if the oil droplet diameter in the ET-35N analysis cell varies from measurement to measurement, a calibration curve for that particular oil droplet diameter is needed to attain accurate concentration readings. For example, if calibration curves for the oil content were based on oil-in-water emulsions containing oil droplets with diameters ranging from 1.3 - 1.7 μ and the oil droplet diameters in the samples analyzed by the ET-35N were to fall near 0.7 μ, the OCM readings would be high by approximately a factor of two.

Oil Drop Diameter (μ)	Slope x 10^3	Correlation Coefficient (R)
0.1	**0.056**	**.991**
0.3	**1.6**	**.993**
0.5	**5.1**	**.997**
0.7	**7.4**	**.993**
0.9	**6.5**	**.988**
1.1	**4.3**	**.985**
1.3	**2.9**	**.985**
1.5	**2.8**	**.984**
1.7	**3.5**	**.982**

Table 2.5.2b. Linear least squares fits to the calculated turbidity versus oil concentration curves shown in Fig. 2.5.2a with the y-intercept fixed at 0 i.e., Turbidity = Slope x Conc. The calculation assumes a uniform oil droplet diameter and spans the concentration range from 0 - 15 ppm for oil-in-water emulsions.

2.5.3 The calculated turbidity vs. concentration curves of Fig. 2.5.2a predict that the ET-35N will not be very sensitive to oil droplets of diameters of 0.1 μ or less. This is demonstrated in Fig. 2.5.3 where the turbidity scale has been expanded to show that oil droplets of 0.1 μ and less do not contribute much to the overall turbidity if droplets of larger diameters are present in the analysis cell. This observation is emphasized by the line in the figure that shows the turbidity that would result from 0.1 μ diameter oil droplets at 30 ppm. This line crosses all the other turbidity curves at concentrations of 1.2 ppm or less. This holds true for a range of oil droplet diameters from 0.3μ to 2.0 μ.

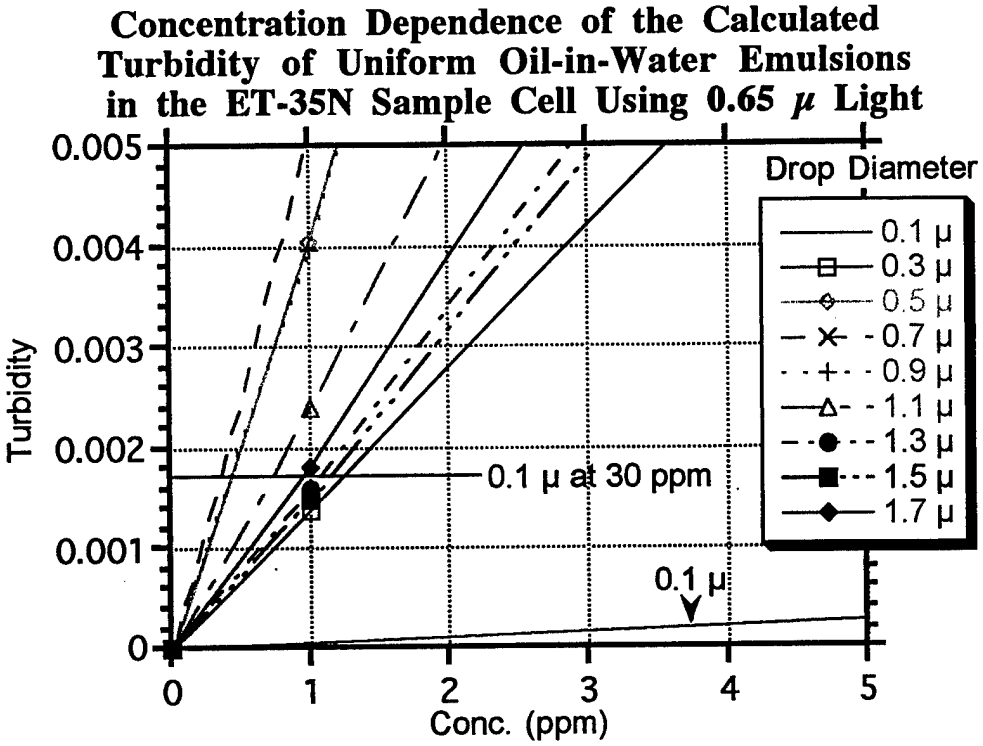

Figure 2.5.3. Calculated turbidity versus oil concentration using Eqn 2.4.4 and based on the optical configuration of the ET-35N analysis cell. The calculations assume a uniform oil droplet size at each droplet diameter.

2.6 Conclusions

2.6.1a Two conclusions regarding increasing the sensitivity of the ET-35N can be made based on the model developed here. They are:

a. Changing the wavelength used to illuminate the sample and repositioning the detector on the OSR will improve the sensitivity of the ET-35N by a factor of approximately three.

b. Incorporating a multiple wavelength light source into the OSR can reduce the sensitivity of the turbidity to the oil droplet size distribution by a factor of two.

2.6.1b Changing the illuminating wavelength to a shorter wavelength will increase the turbidity exhibited by most of the oil droplets in the range of 0.2 μ to 2.0 μ. This is evident from Fig. 2.4.5b where the curve for the turbidity at 0.45 μ incident radiation exceeds that for 0.65 μ radiation except for a range of oil droplet diameters from 0.68 μ to 1.1 μ. In this range of oil droplet diameters the maximum difference in the turbidities is approximately 30%.

2.6.1c The sensitivity of the ET-35N is also improved by moving the 45° detector to an angle substantially higher (>150°) or lower (< 30°) angle than the configuration used in the ET-35N. The calculations show that the turbidity should increase by a factor of two or more (see Fig. 2.4.7a). Moving the detector to a lower angle will move it to a position which will be partially in the "line-of sight" of the LED light source and could interfere with accurate turbidity measurements. Moving the detector to a higher angle does not suffer this drawback.

2.6.2 Incorporating the above enhancements into the existing optical sensor ring (OSR) configuration for the ET-35N imposes some limitations. At present the shortest wavelength LEDs available are near 0.45 μ. Physical limitations of space on the sensor ring limit the increase in the detector angle to about 160°. Using this optical configuration for the sensor ring (see Fig. 2.6.2a), we calculate turbidities that are significantly higher than those calculated for the present ET-35N OSR at all oil droplet diameters from 0.2 μ to 2.0 μ (see Fig. 2.6.2b). The calculated turbidity of the modified OSR is over 15 times higher than that of the ET-35N for oil droplets 0.2 μ in diameter and the minimum improvement in the calculated turbidity for the modified OSR is 2.5 times that of the ET-35N OSR near 1.0 μ. Therefore the model predicts that these changes to the optical configuration of the ET-35N OSR should improve the sensitivity of the turbidity measurements by about a factor of three or better and should bring the detection limits of the ET-35N into the 5 ppm range.

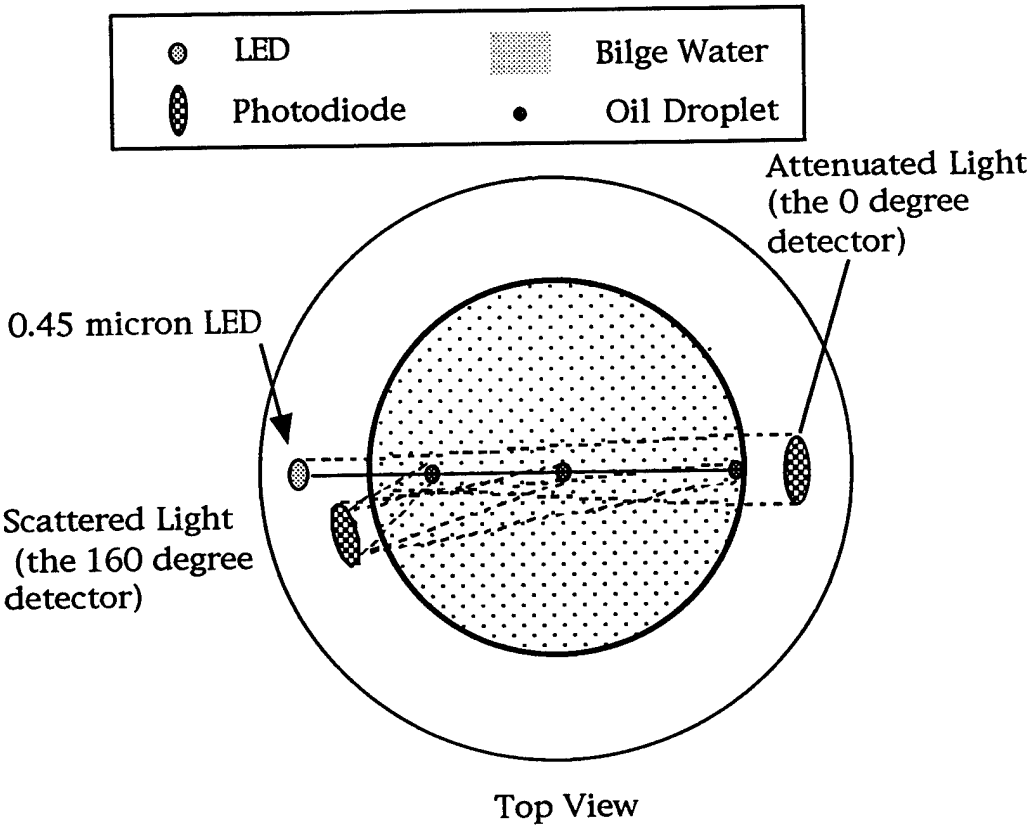

Figure 2.6.2a Schematic of the modified optical sensor ring (OSR) for the ET-35N OCM. The diagram shows the new position of the detector for the scattered light. The other modification is a change in the LED wavelength to 0.45 μ.

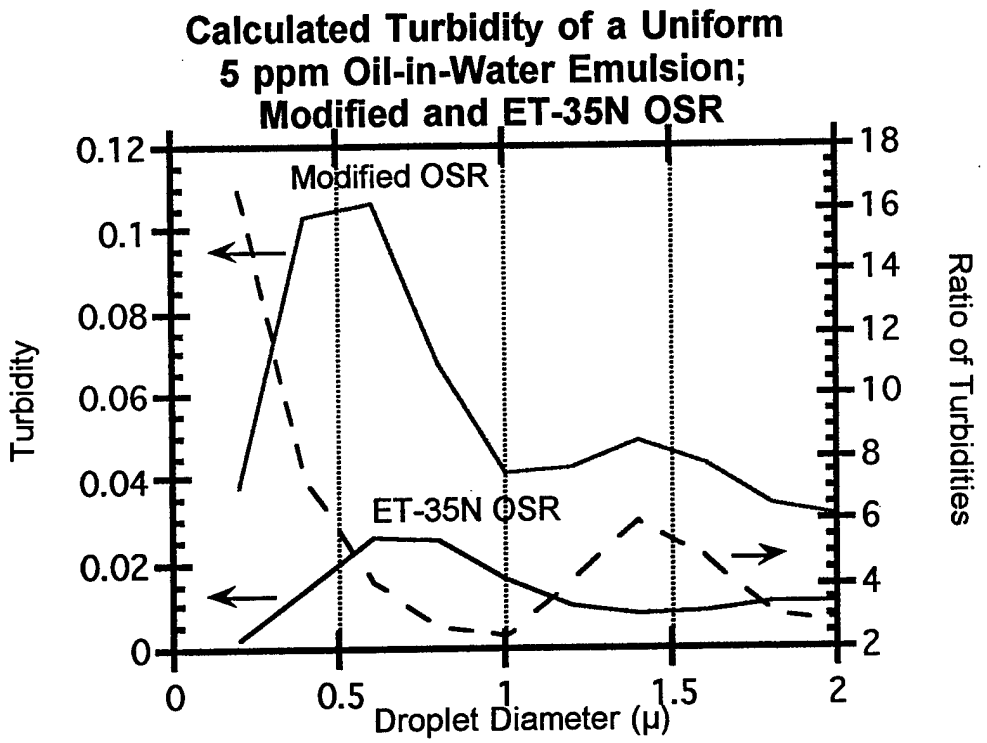

Figure 2.6.2b. Calculated turbidities versus oil droplet size using Eqn 2.4.7a. for the modified optical sensor ring (OSR). The modified (OSR) would have a 0.45 μ LED as a light source and would position the detector for scattered light 160° from the 0° detector. The calculated turbidities for the ET-35N OSR are shown for comparison and the dashed line is the ratio of these two calculated turbidities. The calculations are based on a uniform oil droplet size for each droplet diameter and is for 5 ppm oil-in-water emulsions.

2.6.3 The modified OSR is expected to improve the sensitivity of the ET-35N but it will not reduce the dependence of the turbidity on oil droplet diameter. Oil droplets from 0.4 μ to 0.6 μ will contribute more than twice as much to the turbidity as will droplets from 1.0 μ to 2.0 μ (see Fig. 2.6.2b). One approach to reduce the droplet diameter dependence is to irradiate the sample with multiple wavelengths of light. For example, if two wavelengths of light were used to illuminate the sample, the expression for the turbidity will become

$$T(160)= (I_0(\lambda_1) S(\lambda_1) + I_0(\lambda_2) S(\lambda_2)) / (I_0(\lambda_1) E(\lambda_1) + I_0(\lambda_2) E (\lambda_2))$$

Eqn 2.6.3a,

where S represents the fraction of the light of wavelength λ that is scattered into the 160° detector

$$S(\lambda) = \sum_i \exp(-g(\lambda) l_i) g(\lambda) P(\lambda, \phi_i(160)) / r_i^2 \quad (I=1,150) \quad \text{Eqn 2.6.3b}$$

while E represents the fraction of the light of wavelength λ that is attenuated by the sample as the light traverses the cell and strikes the 0^0 detector.

$$E(\lambda) = \exp(-g(\lambda) l_0 \quad \text{Eqn 2.6.3c}$$

$I_0(\lambda)$ are intensity factors which represent the incident light intensity of wavelength λ that enters the sample and a response function for the detector. The other symbols were defined previously.

2.6.4 Equation 2.6.3a can be used to calculate the turbidity once the wavelengths of the incident light are chosen and values of the I_0s are assumed. Since we wish to reduce the dependence of the turbidity on droplet diameter, we should choose a pair of wavelengths that result in high turbidities for mutually exclusive or nearly mutually exclusive ranges of oil droplet diameters. Referring to Fig. 2.4.7b-2, one obvious choice of wavelengths is 0.45 μ and 1.2 μ. At a wavelength of 0.45 μ, droplets of a diameter of 0.4 μ and 0.6 μ are the largest contributor to the turbidity while at a wavelength of 1.2 μ these droplet diameters are among the lowest contributors to the turbidity. The reverse holds true for droplets with diameters of 1.6 μ and 1.8 μ. These droplets are the lowest contributors to the turbidity at a wavelength of 0.45 μ while being the highest contributors to the turbidity at a wavelength of 1.2 μ. This reversal of contribution to the turbidity (high at one wavelength and low at the other) occurs for most of the oil droplets in the range of diameters studied. A plot of the theoretical turbidity for this choice in wavelengths (assuming that the intensity factors (I_0) are all equal) is shown in Fig. 2.6.4.

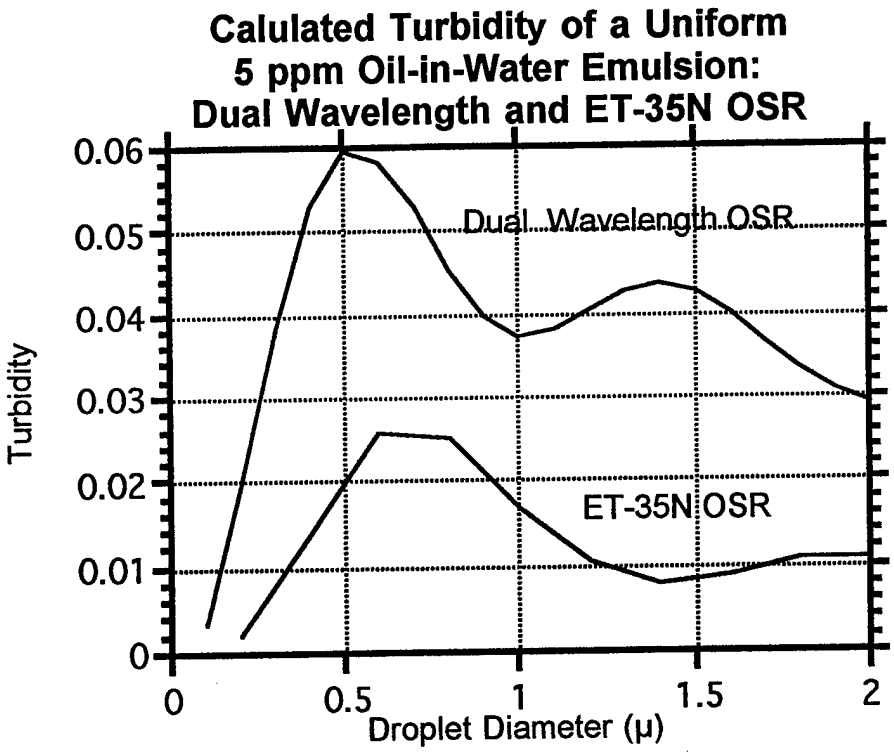

Figure 2.6.4. Calculated turbidities versus oil droplet size using Eqn 2.6.3a. for the modified dual wavelength optical sensor ring (OSR). The modified (OSR) here would have LED or other compact light source emitting at 0.45 μ and 1.2 μ and would position the detector for scattered light 160° from the 0° detector (see Fig. 2.6.2a). The calculations are based on a uniform oil droplet size for each droplet diameter and are for a 5 ppm oil-in-water emulsion

2.6.5 The calculated turbidity for the modified dual wavelength OSR show that the dependence of the turbidity on oil droplet diameter would be reduced. For the modified OSR the ratio of the maximum turbidity to the minimum turbidity is about 1.6 for oil droplet diameters ranging from 0.3 μ to 1.7 μ. For the ET-35N the ration of the maximum turbidity to the minimum turbidity over the same oil droplet size range is about 3.1. This configuration for the OSR is also more sensitive than the ET-35N OSR by about a factor of 2.

2..7 Recommendations

Based on the above calculations it is recommended that:

a. Measurements of ultrasonicted samples from the ET-35N be analyzed with commercial particle sizing instrumentation capable of determining oil droplet

size distributions from 0.1 μ to 5.0 μ to establish the diameter range of oil droplets expected from standards like oil mix #4 and from actual OWS and polisher effluents.
b. A prototype optical sensor ring be constructed with a dual wavelength light source and with the detector(s) at 160° from the corresponding 0° detector(s). That the performance of the OSR be evaluated in a laboratory setting using known emulsions mimicking the particle size distributions measured in the ET-35N sample cell.
c. The computer code used to do the turbidity calculations be modified to increase the flexibility in inputting the optical, geometric and oil droplet parameters and allow more flexibility in the form of the output.

3 Further Modeling Work

3.1 Further reductions in the dependence of the turbidity on oil droplet diameter might be achieved if the I_0 s of Eqn. 2.6.3a were changed. Calculations to test this expectation should be done. In practice changing the I_0 s, can be accomplished by varying the input current (or power) to one of the two emitting elements of the light source thus changing the relative intensity of the light at the two different wavelengths.

3.2 A refinement to the present model would be to introduce an oil droplet size distribution into the turbidity calculations. The present model assumes a uniform oil droplet diameter for each turbidity calculation

3.3 A geometric efficiency factor for the detector could be included in the turbidity model. At present this factor is assumed to be one for all scattered light reaching the detector.

3.4 The present model could be refined to account for the divergence of the light beam from the LED as it travel across the sample cell. The present model assumes that all the scattering droplets are contained in a series of small volume elements distributed along the diameter of the sample cell from the LED to the detector.

3.5 Calculations of the concentration dependence of the turbidity in the modified OSR should be done. It is expected that the slopes of the turbidity versus concentration curves will not exhibit as wide a range as is found in the ET-35N (see Table 2.5.2b).

4 References

1. Influent Maximization 'Saturation' Test on the OPB-10NP Oil/Water Separator System" by R. Morales of Carderock Division, NSWC., Philadelphia Detachment, Sept., 1993.
2. *Light Scattering by Small Particles,* by H. C. van de Hulst, Dover Publications, Inc., New York, NY, p 5, 1981.
3. *ibid,* chapter 9.
4. Subroutines for Computing the Parameters of the Electromagnetic Radiation Scattered by a Sphere, by J. V. Dave, Report No. 320-3237, IBM, Palo Alto Scientific Center, 1968.
5. *Polydisperse Scattering and Its Applications,* by D. Deimendjian, American Elsevier Publishing Co., Inc., New York, NY, p. 74, 1969.

5 Appendix

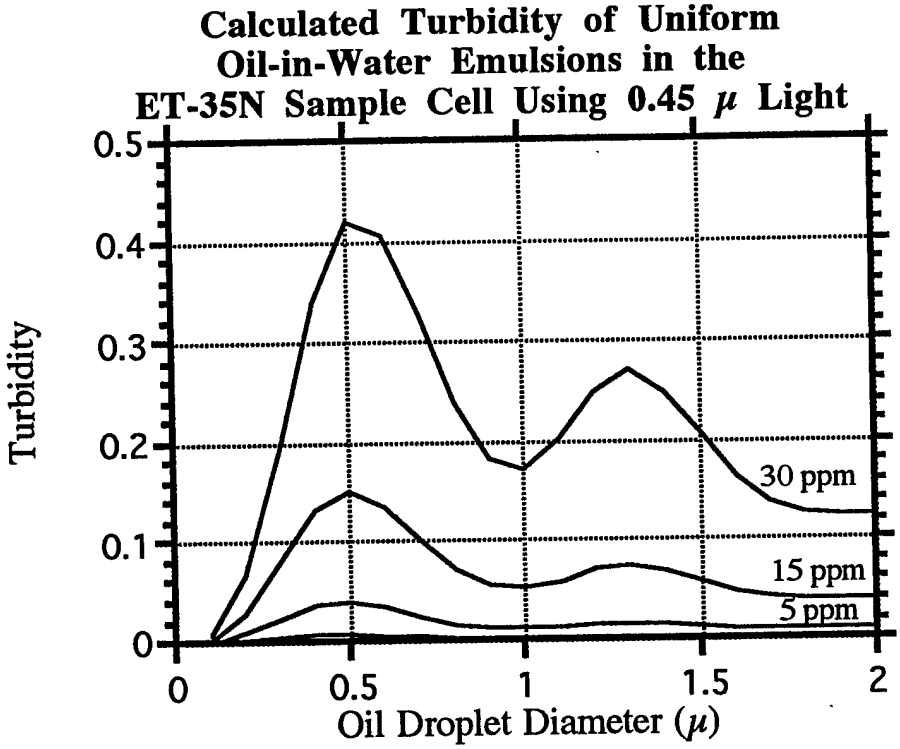

Figure A-1. Calculated turbidity versus oil droplet diameter using Eqn 2.4.4. The calculation is based on a uniform oil droplet size for each droplet diameter and is for 1 ppm (lowest curve), 5 ppm, 15 ppm and 30 ppm oil-in water emulsions.

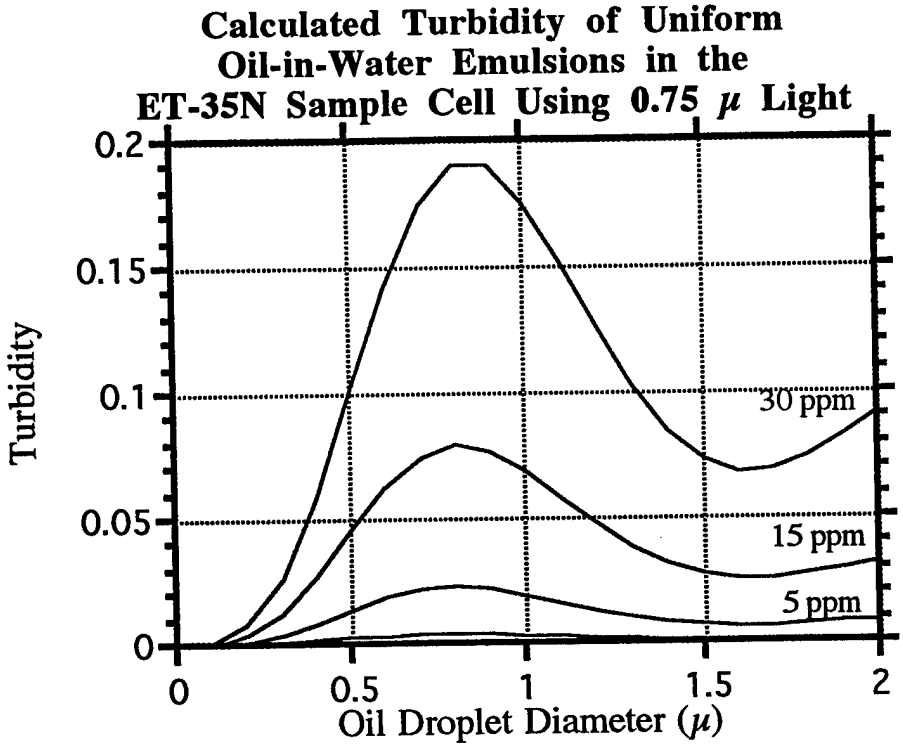

Figure A-2. Calculated turbidity versus oil droplet diameter using Eqn 2.4.4. The calculation is based on a uniform oil droplet size for each droplet diameter and is for 1 ppm (lowest curve), 5 ppm, 15 ppm and 30 ppm oil-in water emulsions.

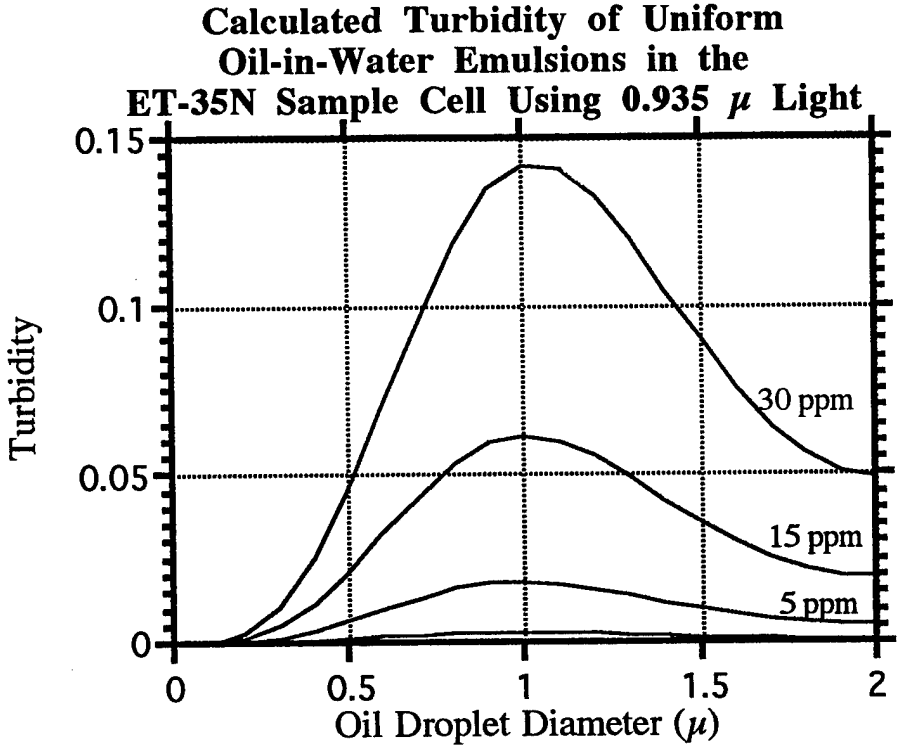

Figure A-3. Calculated turbidity versus oil droplet diameter using Eqn 2.4.4. The calculation is based on a uniform oil droplet size for each droplet diameter and is for 1 ppm (lowest curve), 5 ppm, 15 ppm and 30 ppm oil-in water emulsions.

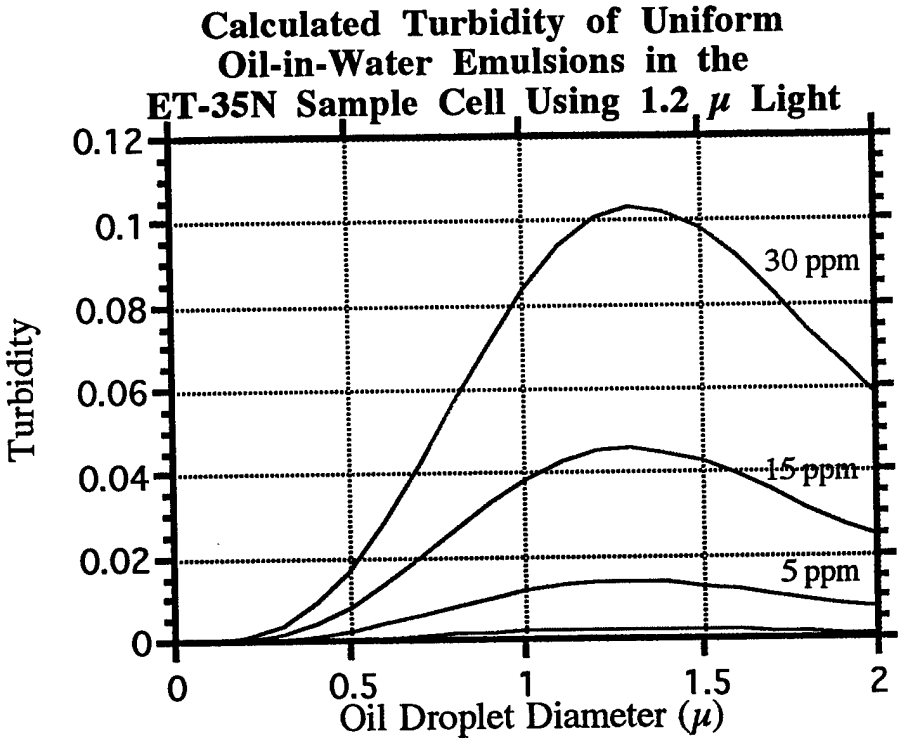

Figure A-4. Calculated turbidity versus oil droplet diameter using Eqn 2.4.4. The calculation is based on a uniform oil droplet size for each droplet diameter and is for 1 ppm (lowest curve), 5 ppm, 15 ppm and 30 ppm oil-in water emulsions.

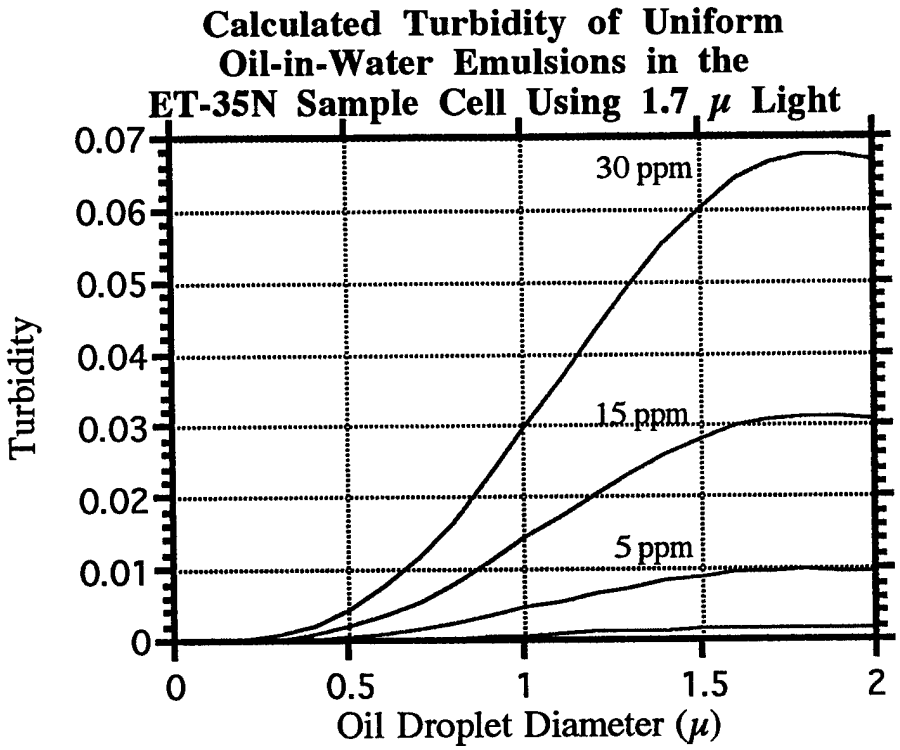

Figure A-5. Calculated turbidity versus oil droplet diameter using Eqn 2.4.4. The calculation is based on a uniform oil droplet size for each droplet diameter and is for 1 ppm (lowest curve), 5 ppm, 15 ppm and 30 ppm oil-in water emulsions.

Calculated Turbidity for 0.45 μ Light Showing Dependence Upon Angle Between the Detectors

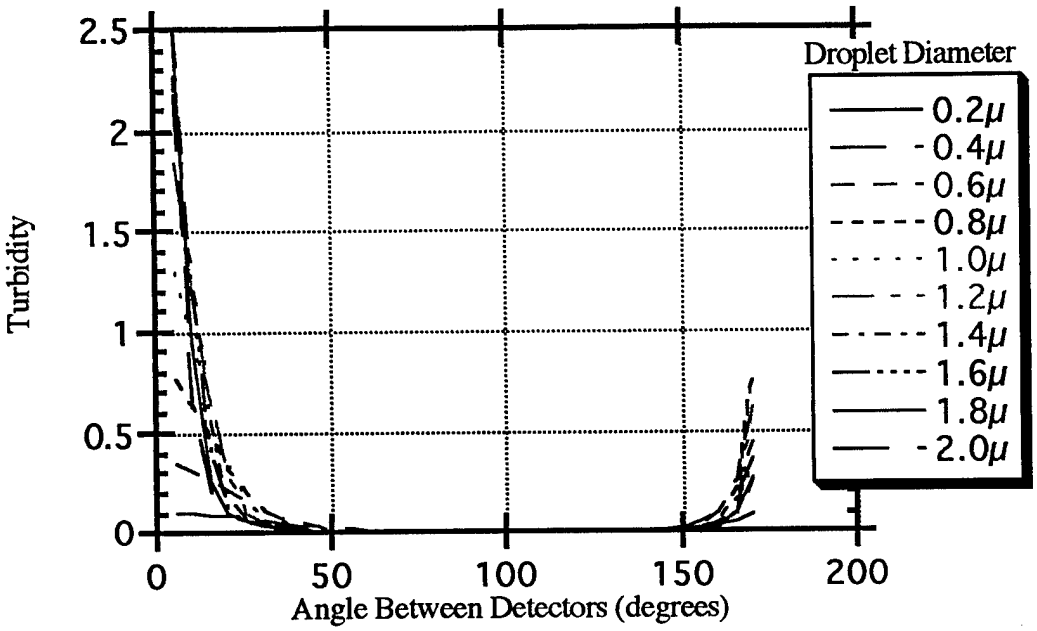

Figure A-6 Calculated turbidity versus angle between the attenuated and scattered light detectors at various oil droplet sizes based on Eqn 2.4.7a. The calculation assumes a uniform oil droplet size for each droplet diameter and is for a 5 ppm oil-in water emulsion illuminated by 0.45 μ light.

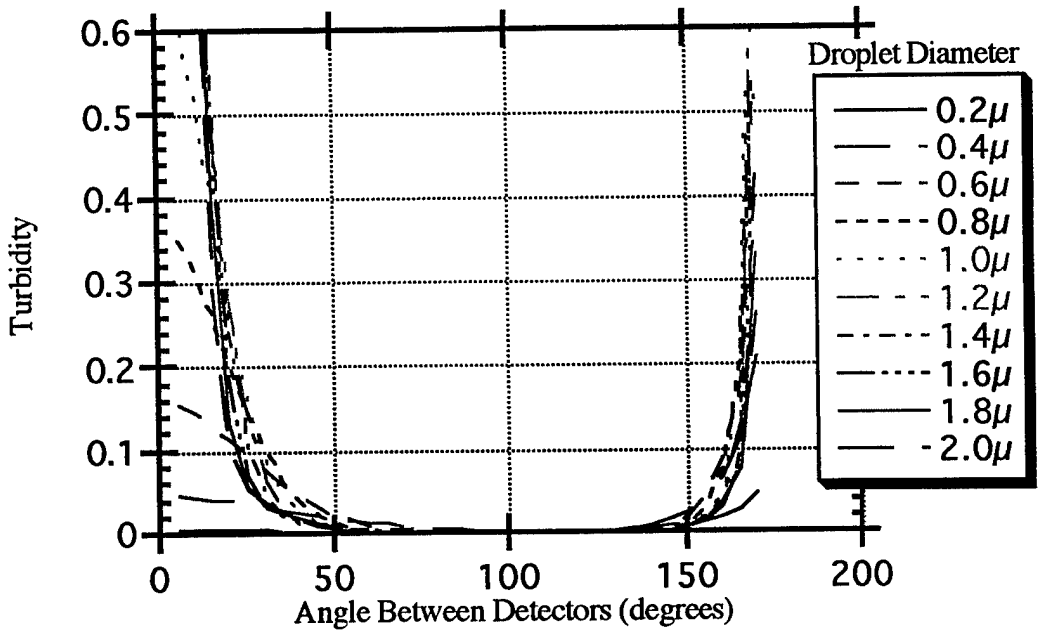

Figure A-7 Calculated turbidity versus angle between the attenuated and scattered light detectors at various oil droplet sizes based on Eqn 2.4.7a. The calculation assumes a uniform oil droplet size for each droplet diameter and is for a 5 ppm oil-in water emulsion illuminated by 0.55 μ light..

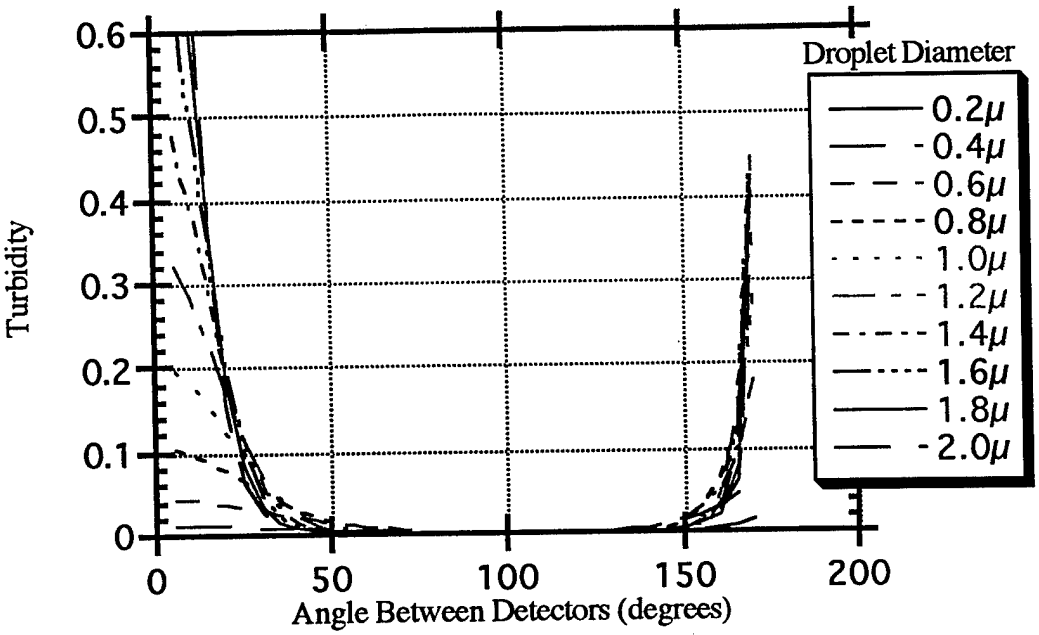

Figure A-8 Calculated turbidity versus angle between the attenuated and scattered light detectors at various oil droplet sizes based on Eqn 2.4.7a. The calculation assumes a uniform oil droplet size for each droplet diameter and is for a 5 ppm oil-in water emulsion illuminated by 0.75 μ light..

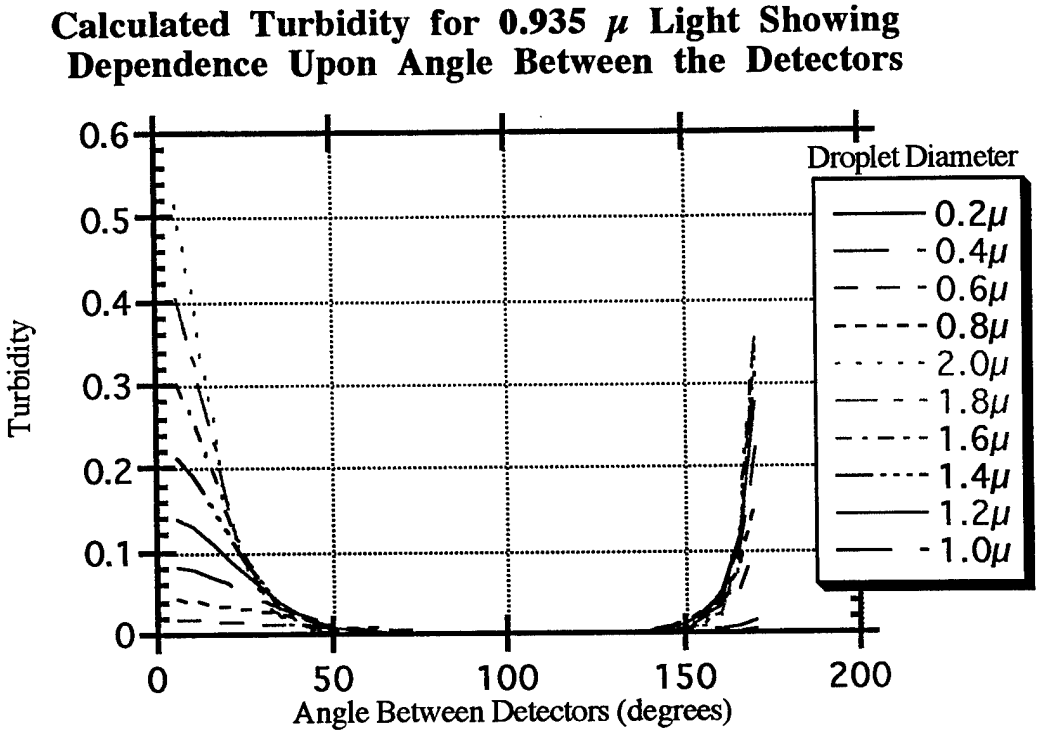

Figure A-9 Calculated turbidity versus angle between the attenuated and scattered light detectors at various oil droplet sizes based on Eqn 2.4.7a. The calculation assumes a uniform oil droplet size for each droplet diameter and is for a 5 ppm oil-inwater emulsion illuminated by 0.935 μ light..

Calculated Turbidity for 1.2 μ Light Showing Dependence Upon Angle Between the Detectors

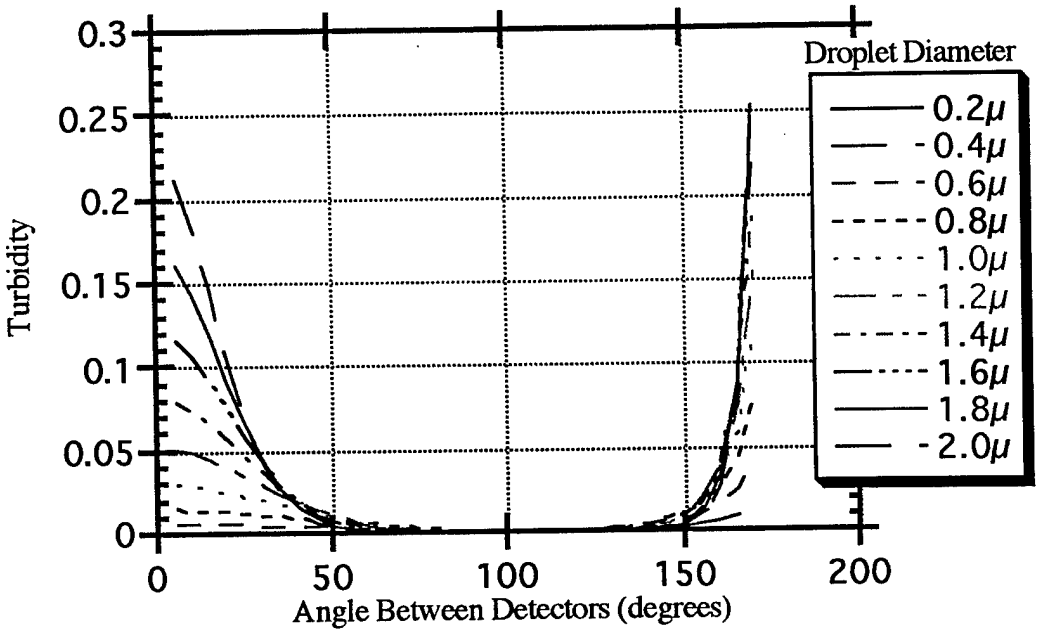

Figure A-10 Calculated turbidity versus angle between the attenuated and scattered light detectors at various oil droplet sizes based on Eqn 2.4.7a. The calculation assumes a uniform oil droplet size for each droplet diameter and is for a 5 ppm oil-in water emulsion illuminated by 1.2μ light..

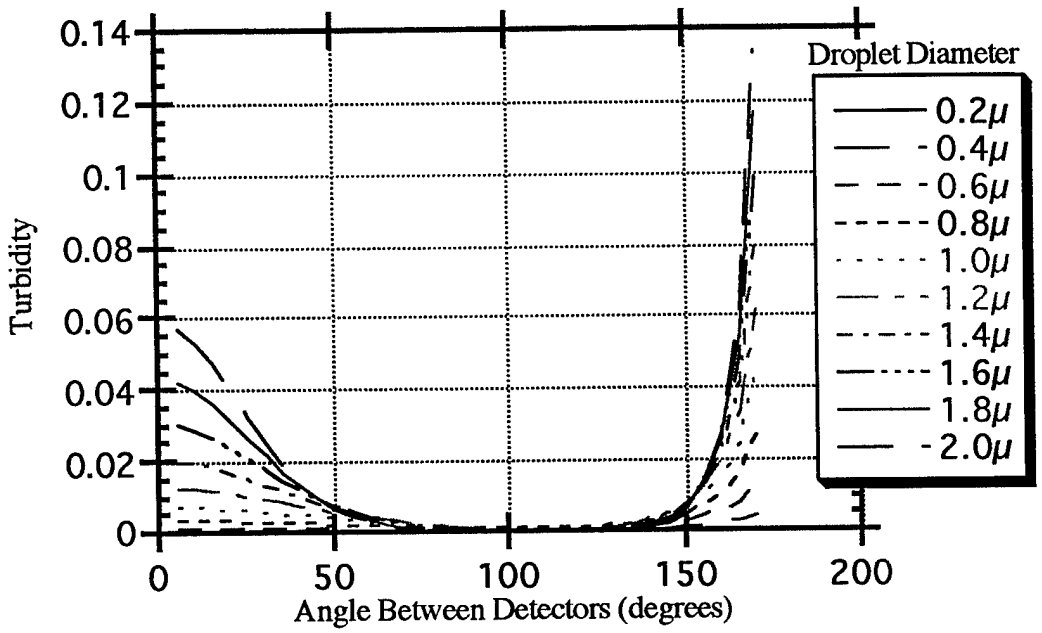

Figure A-11 Calculated turbidity versus angle between the attenuated and scattered light detectors at various oil droplet sizes based on Eqn 2.4.7a. The calculation assumes a uniform oil droplet size for each droplet diameter and is for a 5 ppm oil-in water emulsion illuminated by 1.7μ light..

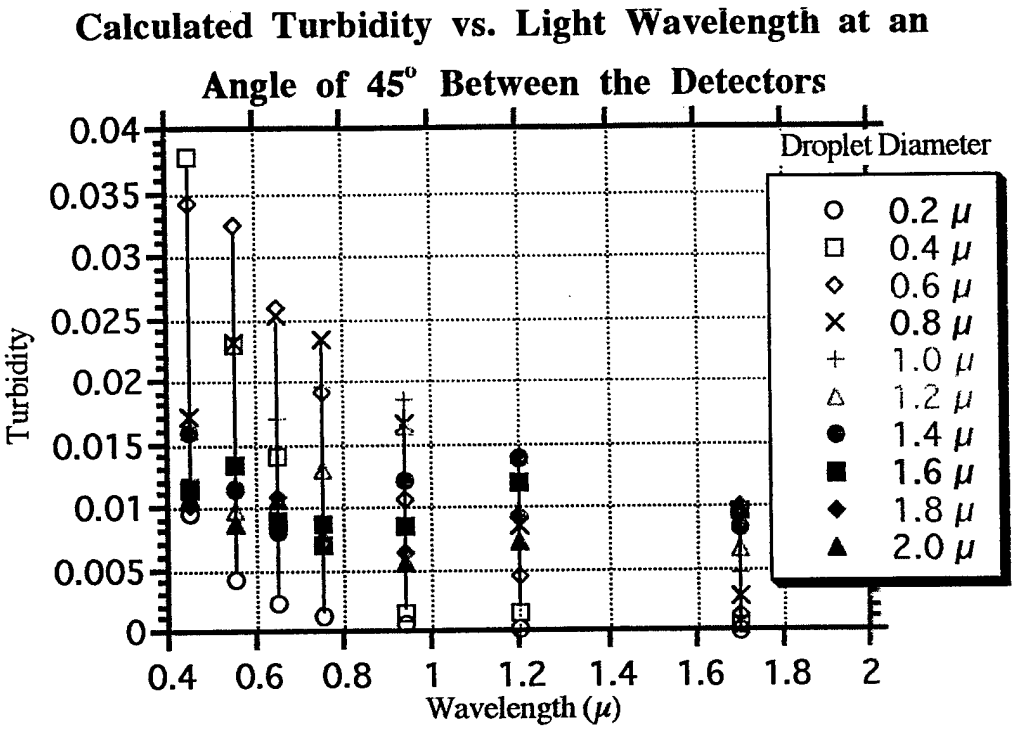

Figure A-12. Calculated turbidity versus wavelength of the illuminating light at a fixed angle between the attenuated and scattered light detectors. The calculation assumes a uniform oil droplet size for each droplet diameter and is for a 5 ppm oil-in water emulsion. An angle of 45° between the detectors is the angle found in the ET-35N OCM.

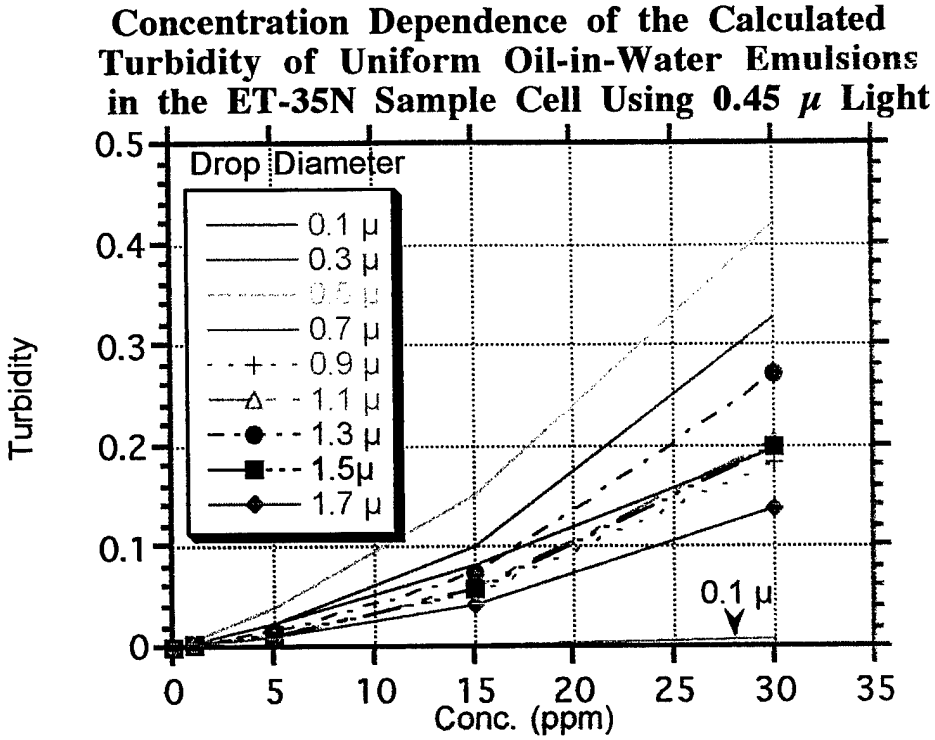

Figure A-13. Calculated turbidity versus oil concentration using Eqn 2.4.4. The calculation assumes a uniform oil droplet size for each droplet diameter and is for 1 ppm, 5 ppm, 15 ppm and 30 ppm oil-in water emulsions.